Spacelabs, Inc.
15521 LANARK ST., VAN NUYS, CALIFORNIA

REPORT NO. SR65-1019

FINAL REPORT

PROPELLANT LEAKAGE DETECTION SYSTEM

CONTRACT NO.
NAS 9-3427

PREPARED FOR:

NATIONAL AERONAUTICS &
SPACE ADMINISTRATION
MANNED SPACECRAFT CENTER
HOUSTON, TEXAS

PREPARED BY:

SPACELABS, INC.
15521 LANARK STREET
VAN NUYS, CALIFORNIA

APRIL 25, 1965

FOREWORD

This report documents the development of the Spacelabs, Inc. Propellant Leakage Detection System. It was prepared under NASA Contract NAS 9-3427.

TABLE OF CONTENTS

LIST OF ILLUSTRATIONS

SUMMARY

29772

A prototype Propellant Leakage Detection System (PLDS) has been developed by Spacelabs for use with bi-propellant reaction control systems. This system was developed under Contract NAS 9-3427 and was delivered to NASA/MSC. The PLDS consists of two sensors and an electronic package. One of the sensors is used to detect propellant leaks in the range from 10 cc/hour to 10,000 cc/hour. The other sensor operates in the range from 1000 cc/hour to 2×10^6 cc/hour. The electronic package provides power and signal conditioning for the sensors. A test unit was included to facilitate testing of the PLDS. The test unit includes a pilot light for the 28 volt power, a high and low range selector switch, a leak alarm indicator light, and test points for monitoring the performance of the PLDS components. The development of the prototype Propellant Leakage Detection System clearly shows that the design and production of optimized systems for flight use is feasible. Figures 1 and 2 show the Propellant Leakage Detection System and test unit.

Author

The experimental program was concerned primarily with development of the flow sensors. Conventional electrothermal flow measuring techniques were investigated and found unsuitable for measuring leakage flow rates of 25 cc/hour. The corrosive nature of the oxidizer, (nitrogen tetroxide), and the thermal instability of the fuel (hydrazine) made absolute sealing of the transducers necessary. After an extensive experimental program, a low flow sensor was devised based on a thermally symmetrical differential temperature measurement technique. A high flow sensor which measures the local heat transfer coefficient on a submerged cylinder was developed for high range leak measurement for O/F monitoring.

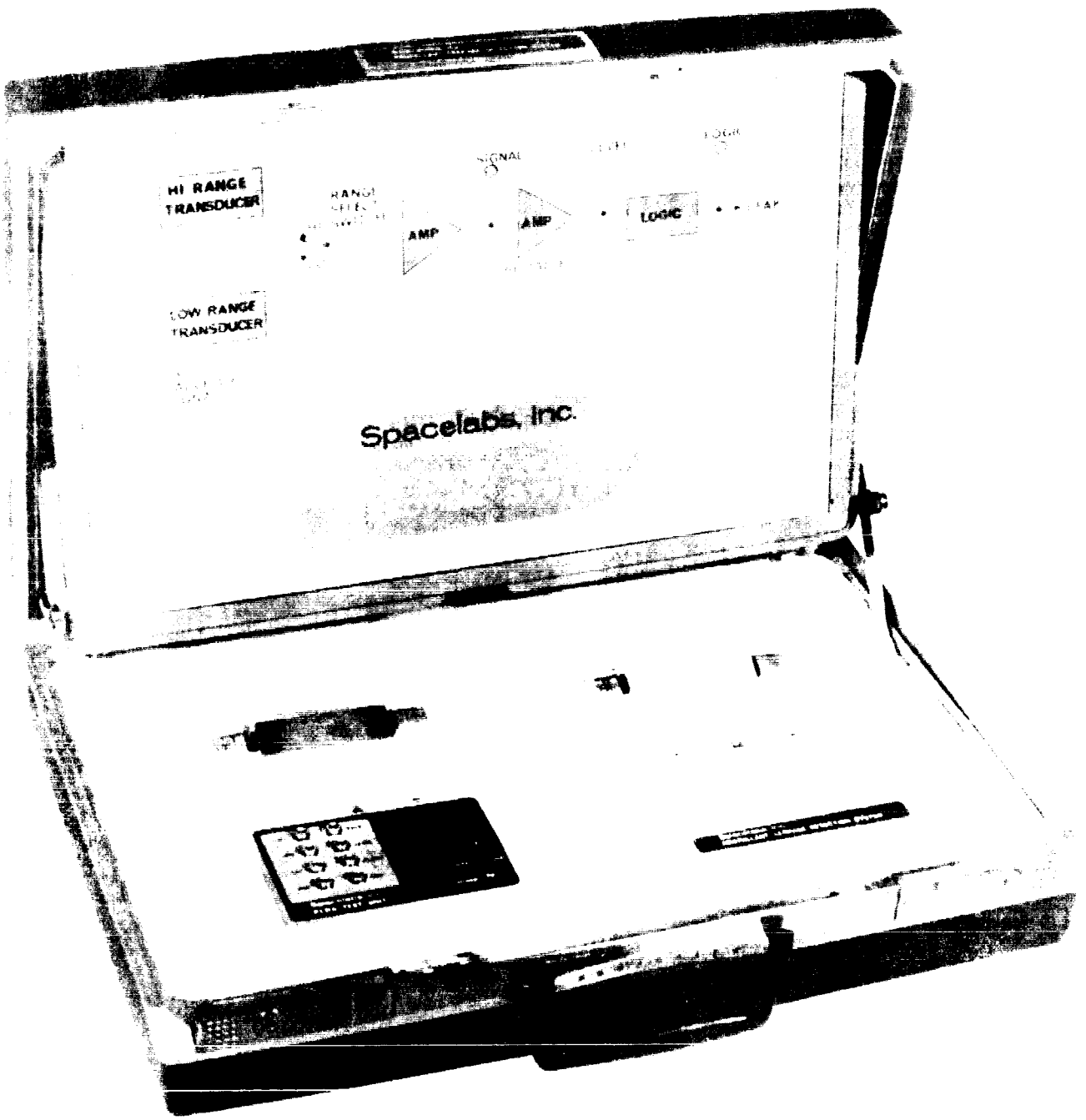
HI RANGE
TRANSDUCER
LOW RANGE
TRANSDUCER
AMP
AMP
LOGIC
Spacelabs, Inc.

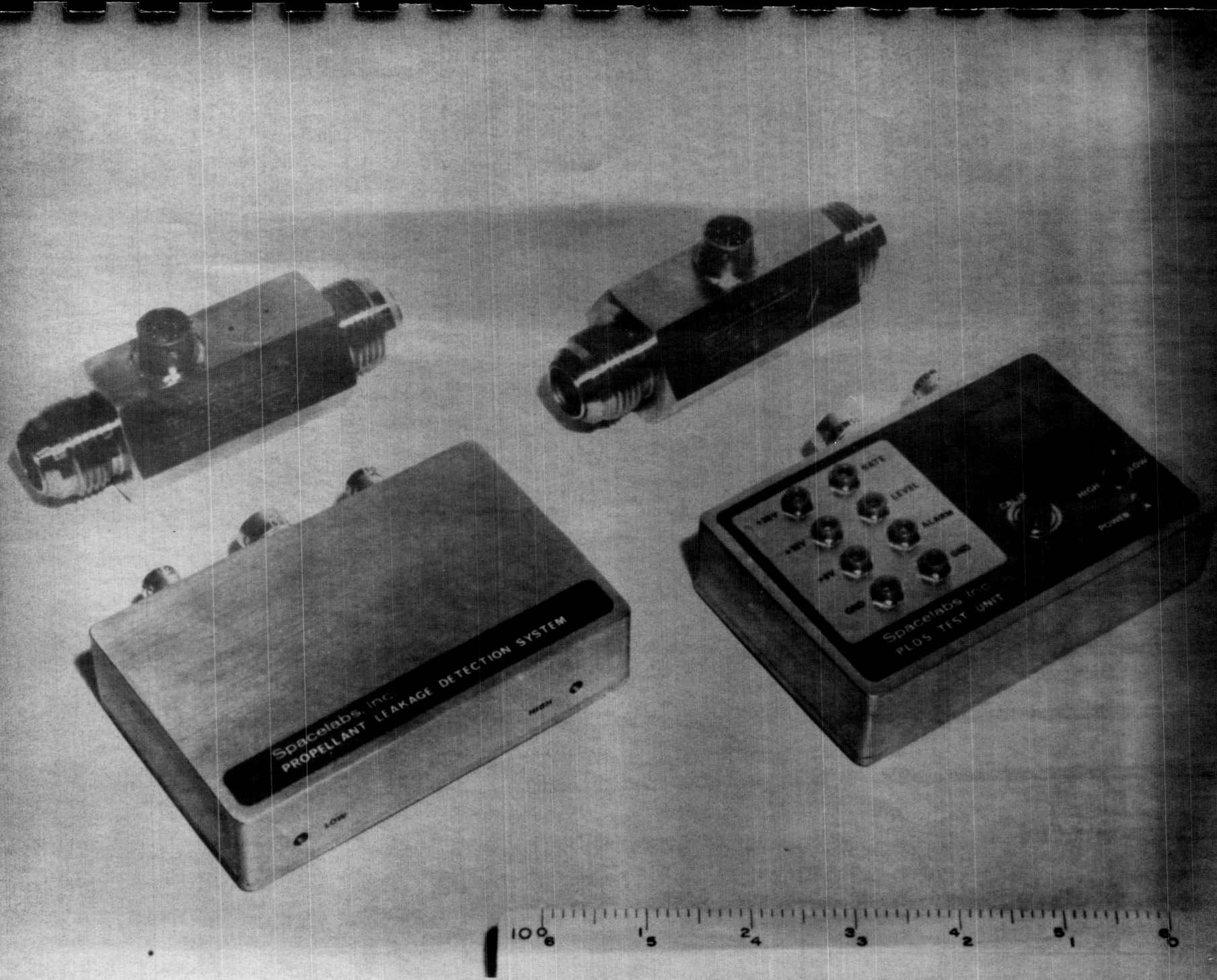

PLDS HARDWARE

FIG. 2

The final configuration of the flow sensors consists of a stainless steel tube 0.6 inches in diameter welded into an outer housing. Standard 3/4-inch fittings are machined on each end of the housing. Smaller stainless steel tubes are mounted across the main flow tube. There are three of these smaller tubes in each sensor. They contain a heater and two thermistors and are secured in place by weldments.

Evaluation tests conducted on the prototype hardware indicate that the system may readily be developed in final form to meet or exceed all performance requirements. The transient response and sensitivity of the prototype hardware are much better than required.

I INTRODUCTION

Space vehicle reaction control systems require monitoring of the propellant flow. Propellant leakage of extremely small magnitude can exhaust the propellant supply during an extended space mission. A system failure such as valve malfunction or line rupture could result in the loss of a significant quantity of propellant in a matter of seconds. Either of these problems might be corrected by emergency procedures if prompt action were undertaken. A suitable propellant monitoring system would detect extremely small leakage rates and would indicate the presence of unusually high propellant utilization rates requiring immediate attention. A further desirable characteristic in a propellant monitoring system would be the ability to detect abnormal O/F ratio during operation of the reaction control system.

The leakage detection problem differs markedly from ordinary flow measurement. The leakage flow velocities are extremely small. Normal flow velocities generally lie between 0.1 ft/sec and 10 ft/sec. In contrast, at 20 cc/hour the flow velocity through a pipe 0.6" in diameter is 10^{-4} ft/sec, or 1/3 ft/hour. A corresponding dynamic head is 1.6×10^{-10} ft. This is far below the range of conventional flow measurement techniques.

Another problem arises from the corrosive nature of the propellants. Nitrogen tetroxide is an extremely active oxidizer which attacks all but a few materials of construction. Hydrazine and its derivatives are thermally unstable and are susceptible to catalytic decomposition. They can be permitted contact with only a limited group of materials.

The problems of propellant monitoring for a reaction control system led to a program directed at feasibility investigation and development of a suitable Propellant Leakage Detection System. This program was undertaken under NASA Contract NAS 9-3427 between the NASA/Manned Spacecraft Center and Spacelabs, Inc. The objectives of the program are set forth in Section II. The development program is outlined in Section III. The design and fabrication of the final hardware are described in Section IV. The results of evaluation tests of the prototype hardware are presented in Section V. Section VI summarizes the findings of the program and presents recommendations for future activities.

II OBJECTIVES OF THE PROGRAM

The primary program objective was to develop and demonstrate the feasibility of a prototype Propellant Leakage Detection System. The program was aimed at the generation of sufficient knowledge to enable the design and fabrication of a full-scale optimized system under a later program. The prototype system was to include leakage detection devices, control electronics, and a leak alarm sub-system. The system requirements are presented in Exhibit A of Contract NAS 9-3427, and are summarized below.

A. Reaction Control System Characteristics

A typical reaction control system is shown in Figure 3. It consists of a propellant supply system, a propellant leakage detection system, and a number of rocket motor assemblies. The propellants are nitrogen tetroxide and members of the hydrazine family of fuels. These include hydrazine, monomethyl hydrazine (MMH), and unsymmetrical dimethyl hydrazine (UDMH).

The operating pressure level of the system ranges from 100 to 300 psi. Normal operating temperatures are from 20° F to 85°F. Normal flow rates range from 0.22 #/sec to 0.88 #/sec for oxidizer, and from 0.11 #/sec to 0.44 #/sec for fuel. The nominal O/F is 2.0. Nominal line diameters are 3/4-inch for the oxidizer and 5/8-inch for the fuel.

Two modes of thrust chamber operation are used. In the steady mode, the engine may fire continuously for up to 10 minutes. In the pulse mode, the engine operates in pulses as short as 20 milliseconds.

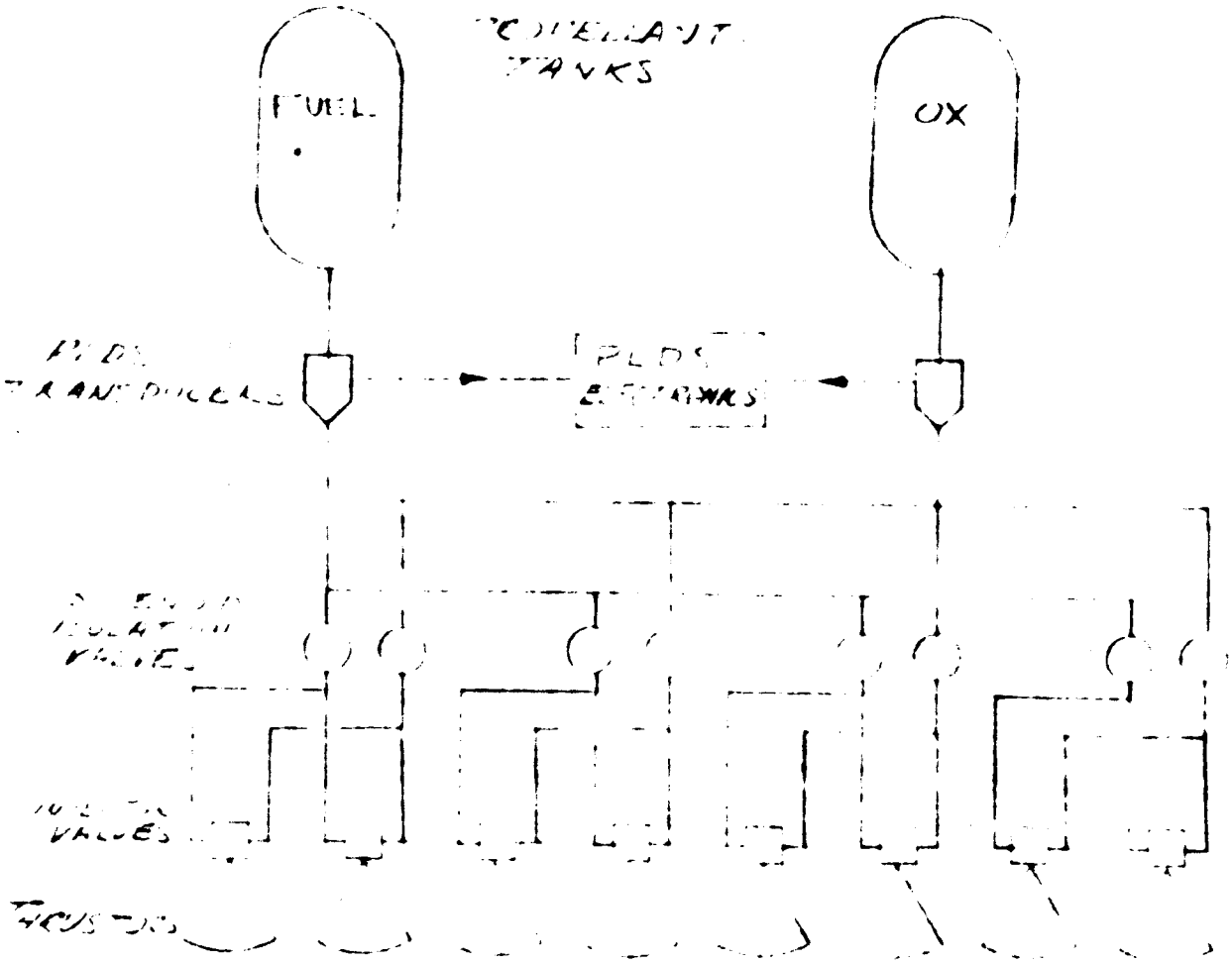

REACTION CONTROL SYSTEM

FIG. 3

B. Propellant Leakage Detection System Characteristics

The performance requirements for the Propellant Leakage Detection System include low flow leakage detection, high flow leakage detection, and flow monitoring.

Low Flow System

The low flow detection system is intended for intermittent operation. Whenever it is desired to check for low flow leakage, the low flow system will be activated. The system must indicate the presence of any leakage rate between the threshold of the low flow system and the threshold of the high flow system. The threshold of the low flow system is 25 cc/hour for the fuel and 35 cc/hour for the oxidizer. The allowable power consumption for the low flow system is 25 watts of 28 volt d. c. power during the 10 minute operating period.

High Flow System

The high flow warning system is intended for continuous operation (except during low flow leakage checks). It is to provide a warning in the event of a malfunction which requires immediate attention. When the RCS is not operating, such a malfunction is defined as a leakage rate exceeding 1350 cc/hour of fuel or 1700 cc/hour of oxidizer. It must respond to such a leak before 66 cc of fuel or 75 cc of oxidizer have passed the detector. The high flow system should also provide an alarm when the RCS is operating and the O/F ratio falls outside of the range from 1.0 to 2.0. The power used by the high flow system is not to exceed 5 watts.

General Characteristics

The PLDS must be integrated into the propellant lines of the reaction

control system so as to cause no interference with normal operation. The materials of the PLDS sensors must be compatible with the propellants. The flow sensing elements must introduce a pressure drop less than 1% of system operating pressure at the maximum expected flow rates. The system must provide high reliability and must be fail-safe with respect to the reaction control system. No failure in the PLDS can compromise the reliability of the reaction control system.

C. Environment

The PLDS must operate in the same environment as the RCS. The environmental requirements for the system are presented in Appendix A. These include acceleration up to 8.5 G, shock up to 15 G, random and sinusoidal vibration, and normal radiation requirements for interplanetary space travel. The high flow warning system will be used when the attitude control system is firing and angular acceleration of the spacecraft may occur. For use of the low flow warning system, external disturbances to the system will be minimized. The environmental factors outlined in Appendix A do not form specific requirements for the breadboard hardware which was delivered under the present program. Testing was limited to successfully demonstrating the feasibility of future development of qualified hardware.

III LEAK METER DEVELOPMENT PROGRAM

Following receipt of the contract, a development program was initiated to meet the contract requirements. Consideration was given to the use of standard electrothermal flowmeter techniques. Spacelabs, Inc. has for a number of years developed and manufactured electrothermal flowmeters which rely on the measurement of wall heat transfer in a tube. This is done by measuring the electrical power required to maintain a portion of the tube a fixed temperature difference above the incoming stream. This type of flow sensor has proved very satisfactory for relatively low flow measurements in the past.

A closer examination of the requirements revealed some problem areas. It appeared that the power consumption was too high at the flow rates encountered during high flow monitoring. The design of conventional electrothermal flowmeters could not easily be modified for propellant compatibility. Calibration difficulties were expected at the low flow threshold. Heat leakage due to conduction and free convection would tend to completely dominate the leakage signal under ground testing conditions even though the problems of free convection would disappear in space. Preliminary water flow tests conducted with Spacelabs' flowmeters confirmed the existence of these problems and led to a search for more suitable low flow measuring techniques.

The solution to the problems discussed above lay in two different directions. At high flow rates, the primary problem was one of reducing the magnitude of the power required while simultaneously providing isolation of the electrical elements from the propellants. The solution to these problems was the use of a smaller heat source which could be inserted into the stream to provide a significant temperature signal at a reduced power level. The solution to the low flow sensing

problem was a system which in ground calibration and checkout would be sensitive only to the leakage flow. Such a goal could be achieved by the use of two sensors arranged to provide thermal symmetry for all effects except those due to flow.

These initial concepts led to a combined analytical and experimental investigation which ultimately resulted in the development of satisfactory low flow and high flow sensors.

A number of analytical studies were conducted during the PLDS development program. The most significant of these studies are attached to this report in Appendix C. The first of these was concerned with an evaluation of the heated wall flowmeter for application to the Propellant Leak Detection System. When it became apparent that power consumption at RCS flow rates would be excessive while the low flow signal might be dominated by stray heat losses, an analysis was conducted of a thermal differential transducer using temperature sensors and a heat source submerged in the fluid. This analysis indicated that a satisfactory low flow sensor could be developed utilizing this technique. The analysis also indicated that a thermal differential sensor would not be suitable for O/F monitoring.

The high flow sensor developed is identical in principle to Spacelabs' heated wall flowmeters. The primary difference is that the PLDS high flow sensor measures the heat transfer coefficient at the leading edge of a small cylinder while the heated wall meter measures the heat transfer coefficient at the wall of the main flow tube. The total heated area exposed in the cross tube sensor is greatly reduced compared to the heated wall system. An analysis of the conversion factors between propellant flow rates and equivalent water flow rates was performed to determine the range of water flows to be used in system evaluation testing.

The details of the experimental program directed at the development of the sensors are presented in Appendix B. The first configuration tested was found inadequate because of the low temperature rise achieved at the sensors. The possibility of using self-heated thermistors was considered and preliminary heat transfer tests with single thermistor beads were conducted. The results of these tests showed two interesting features. At higher flow rates, the thermistor beads behaved as predicted by laminar flow heat transfer theory. However, at very low velocities, heat transfer from the beads was controlled by free convection. The free convection was found to greatly reduce the temperature of the sensors when they were placed too far from the heat source. In subsequent tests, the sensors were moved closer to the heat source and the heater power was increased. It was felt that the thermal differential sensor would meet the PLDS requirements if some means could be found for encapsulating the flow elements to remove them from contact with the stream. This led to the first cross-tube thermal differential flowmeter tests. These were extremely encouraging and indicated an adequate signal level at the low flow threshold. Further tests of the cross-tube flowmeter clearly indicated that this should be the system used for low flow leak detection. The performance of the thermal differential flowmeter at high flows was as expected. The flowmeter provided an adequate signal at the threshold of the high flow warning system. The signal then decreased at higher flows as the cooling effect of the fluid lowered the heater temperature.

Preliminary high flow tests were conducted using a heated wall meter very similar to the "standard" Spacelabs flowmeter. The tests indicated that the sensor provided a good flow measurement, but (as had previously been determined analytically) the power input required at high flows was excessive. The final high flow configuration tested was a three-element cross-tube system in which

the elements of the heated wall sensor were replaced by corresponding elements in the cross-tubes. The upstream sensor was replaced by an upstream tube containing a bead thermistor. The heating element around the wall was replaced by a heating element in a cross-stream tube. The temperature sensing element at the heated wall was replaced by a temperature sensing element in a cross-stream tube which was thermally and mechanically bonded to the upstream edge of the heating element tube. This configuration was found to give far greater sensitivity at much lower input powers than the heated wall sensor. It could also be easily fabricated in a propellant compatible version. This configuration was therefore selected as the one to be used for the flow sensor. Figure 4 shows some of the breadboard sensors tested in the course of the experimental program. After the preliminary screening experiments had led to a selection of sensors for the low flow and high flow requirements, an experimental test item was fabricated which contained low flow and high flow sensing elements in a 3/4-inch diameter stainless steel tube. Tests were conducted in the water flow facility using both low temperature and high temperature water to examine the effect of changing fluid properties on the performance of the sensors. The high flow performance was relatively unaffected by changes in fluid temperature. The low flow sensor showed a drop in sensitivity at high fluid temperatures. This was due to the change in free convection characteristics within the sensor and will be much less pronounced under zero-G conditions. Particular attention was directed at the effects of free convection and fluid temperature on the behavior of the low flow sensor. At low heater power, increasing the heater power provided increased sensitivity at low flow rates. As the heater power was further increased, the sensitivity reached a maximum and began to drop. This was found to be due to free convection around the heater element. When the vertical free convection

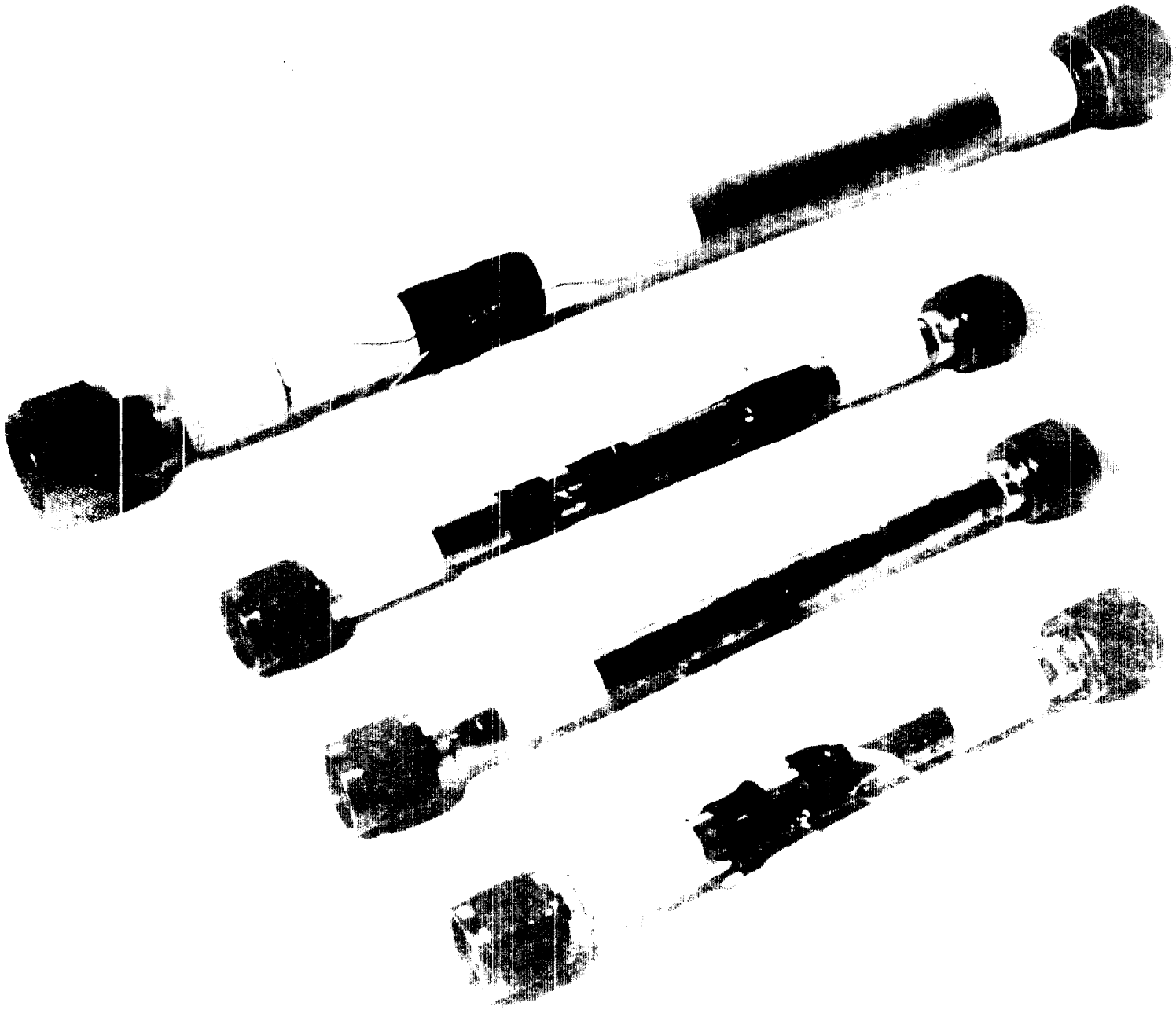

velocity around the heater element is comparable in magnitude to the flow velocity, the sensitivity of the instrument begins to fall. As the velocities associated with free convection are increased by increasing heater power, the sensitivity of the instrument decreases rapidly. The presence of these free convection effects tends to degrade the sensor performance. The zero leakage indication is unaffected by convection because of the symmetry of the instrument. However, the sensitivity at low flow rates is greatly reduced. This is undesirable because sensors are most easily evaluated in a normal 1 G environment.

Minimization of free convection phenomena was achieved by use of flow baffles parallel to the normal flow direction. These baffles interfere with the convection eddies and break up the free convection process. A number of fairly elaborate baffle configurations were considered and discarded in favor of an extremely simple V baffle which was tested and adopted for the final model. With the V baffle in place, the sensitivity of the instrument near the low flow threshold was greatly increased.

The final design of the prototype flow sensors and electronic circuitry is described in Section IV of this report. Tests of the complete system are described in Section V and indicate that the program was successful.

IV DESIGN OF FINAL HARDWARE

A. Sensor Design

One of the major objectives of the experimental program was the development of a flow measuring technique in which all the sensor components could be enclosed by stainless steel. The final transducers were designed to take advantage of the success of this facet of the experimental program. Although the sensing elements for both high range and low range operation could be housed in a single sensing package, (as they were in the final experimental transducer tested), it was decided to fabricate separate low and high range transducers to provide versatility and to simplify manufacturing and testing. Both transducers were fabricated from type 304 stainless steel with all internal joints welded together. This construction technique was selected after material studies had pointed out the unavailability of any completely satisfactory non-metallic sealing materials.

The designs for the transducers are shown in Figures 5 through 8. The transducers consist of an inner tubing assembly and an outer housing. The inner tubing assembly consists of a 5/8" outer diameter, 0.020 wall welded and drawn tube in which smaller tubes containing the heaters and thermistors are mounted across the stream. The smaller tubes are held in place by welding their ends to the walls of the 5/8" tube. Some initial difficulty in making suitable welds by standard arc welding techniques was circumvented by employing laser welding. Figures 9 and 10 show the partially assembled low and high range transducers. The laser welds are visible through the circular holes in the outer housings.

After welding the inner tubing assemblies together, they were slipped into the outer housing and welded in place using the tungsten-inert gas process. Figure 11

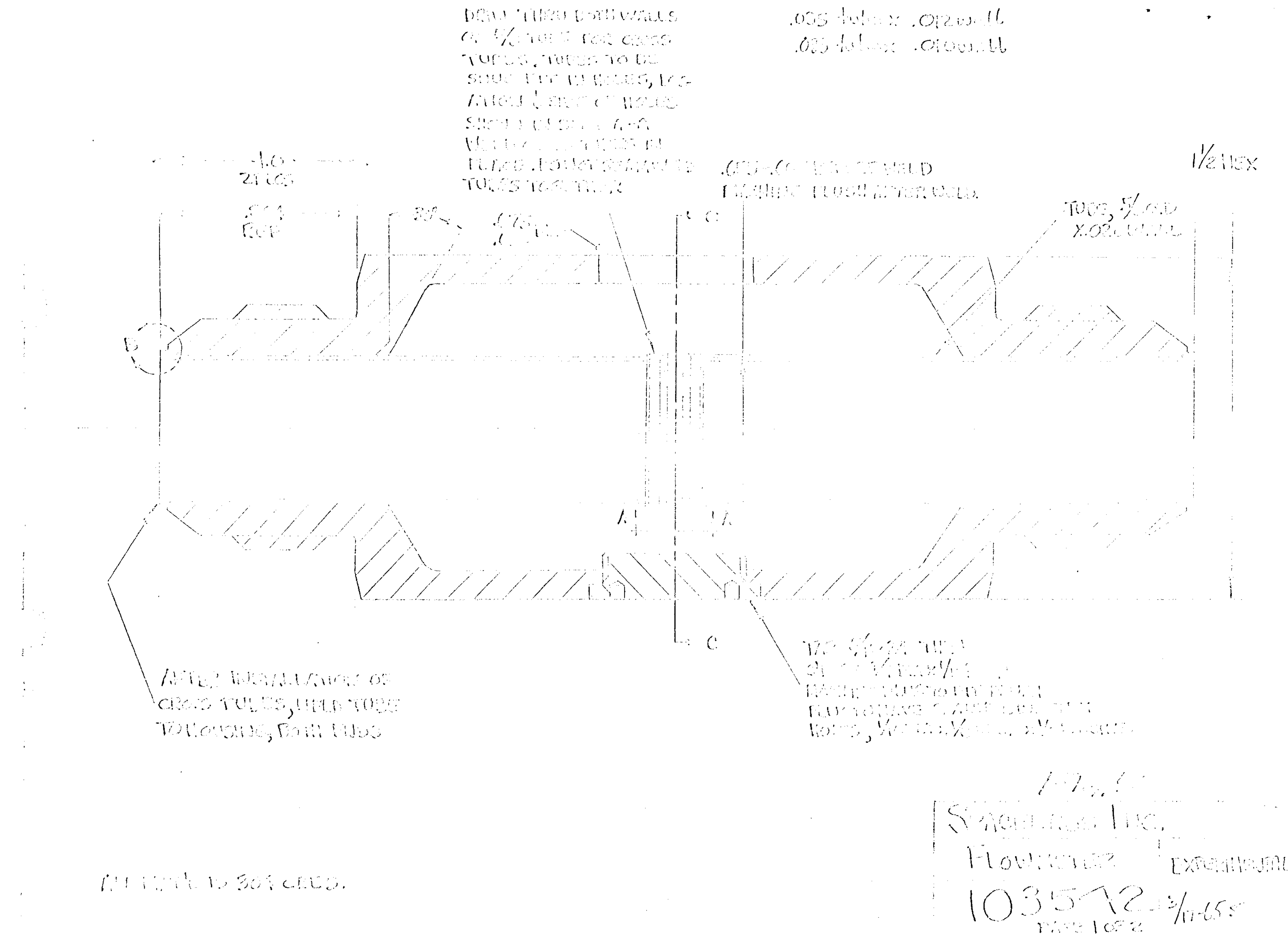

1/2 HEX
C
C
A
A
B
AFTER INSTALLATION OF CROSS TUBES, WELD TUBE TO COUPLING, BOTH ENDS
FLOWMETER
EXPERIMENTAL
103572

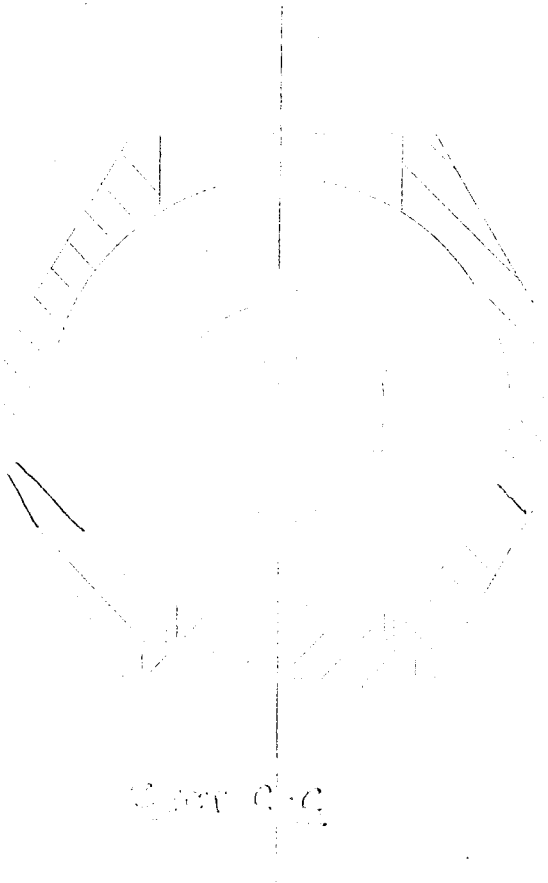

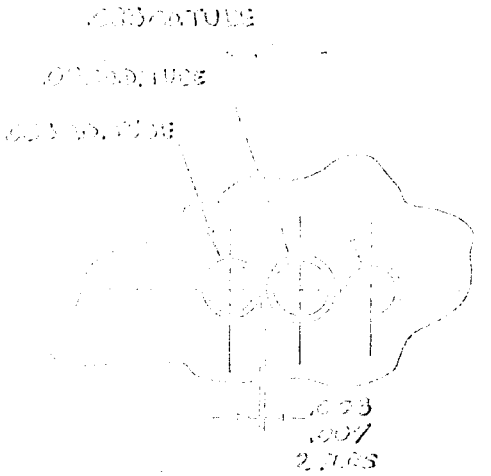

SEC A-A

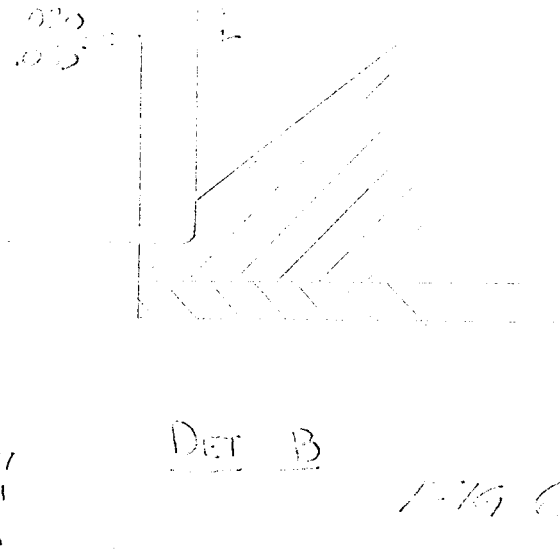

DET B

SPACELABS INC.

FLOWMETER

1035542

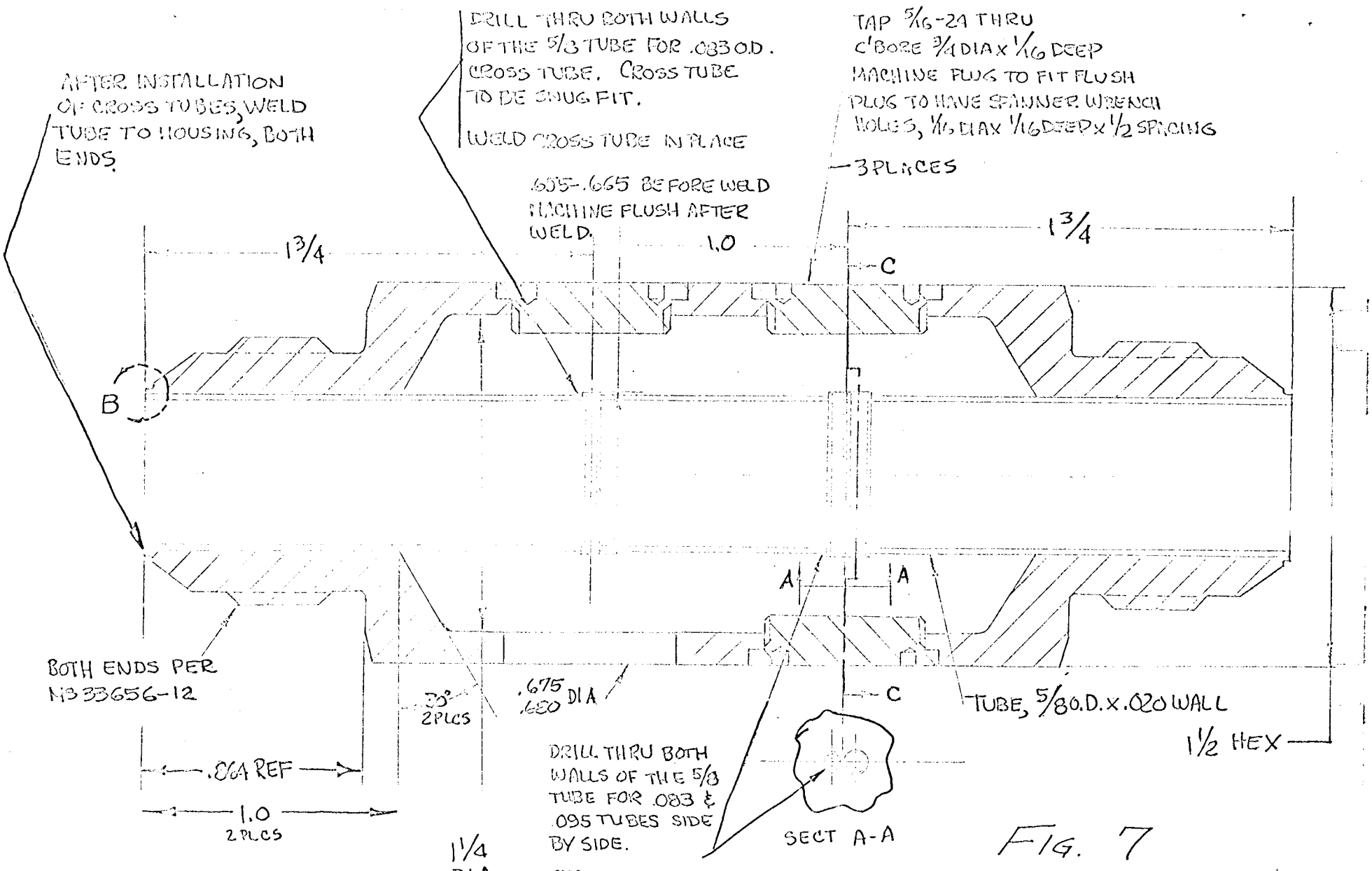

ALL MAT'L IS 304 CRES

FIG. 7

SPACELABS INC.	
FLOWMETER	EXPERIMENTAL
103543 PAGE 1 OF 2	3/11/65

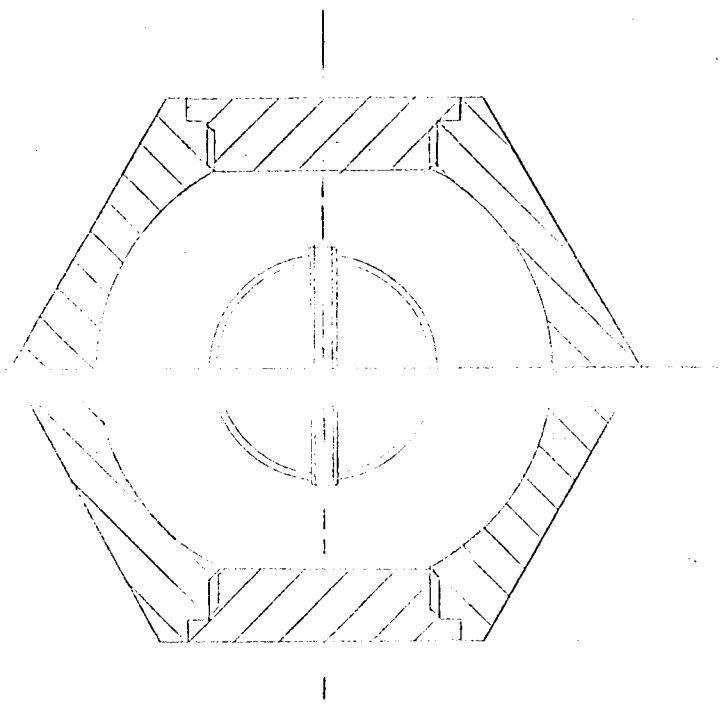

SECT C-C

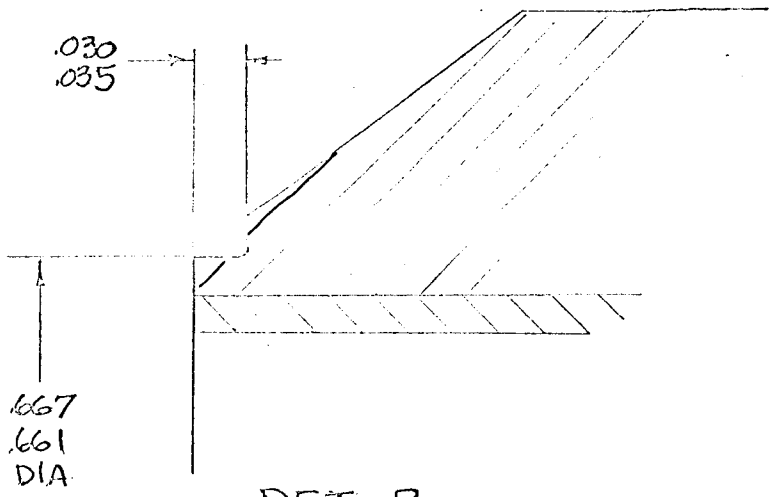

DET B

FIG. 8

SPACELABS INC.
FLOWMETER
103543 PAGE 2 OF 2

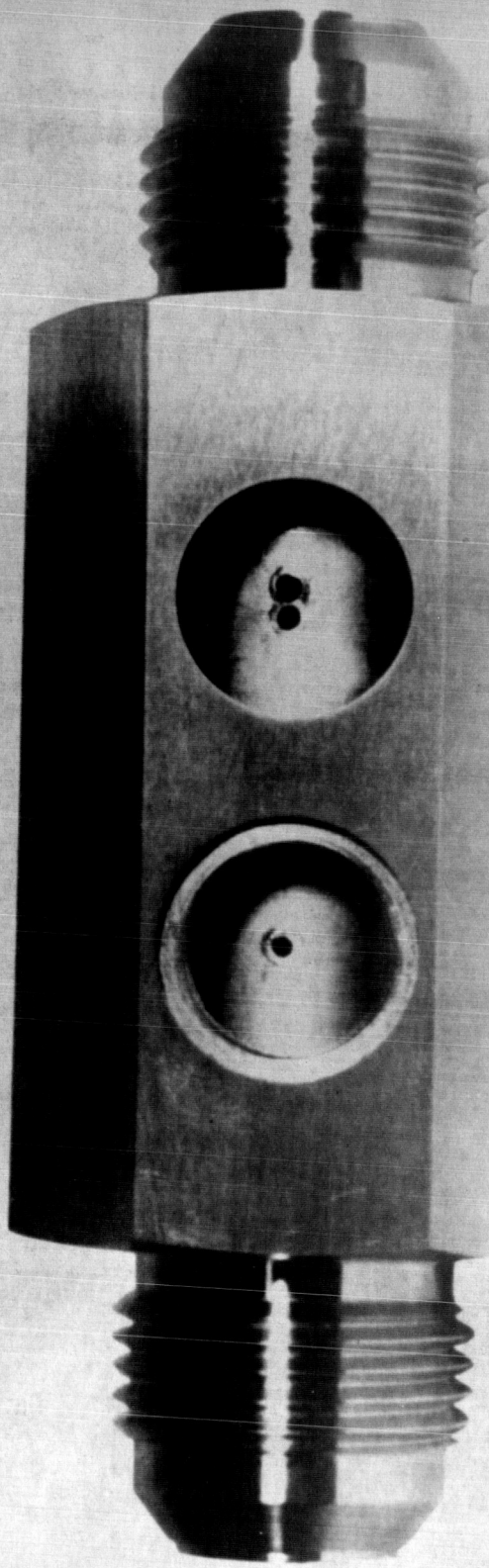

HIGH RANGE TRANSDUCER

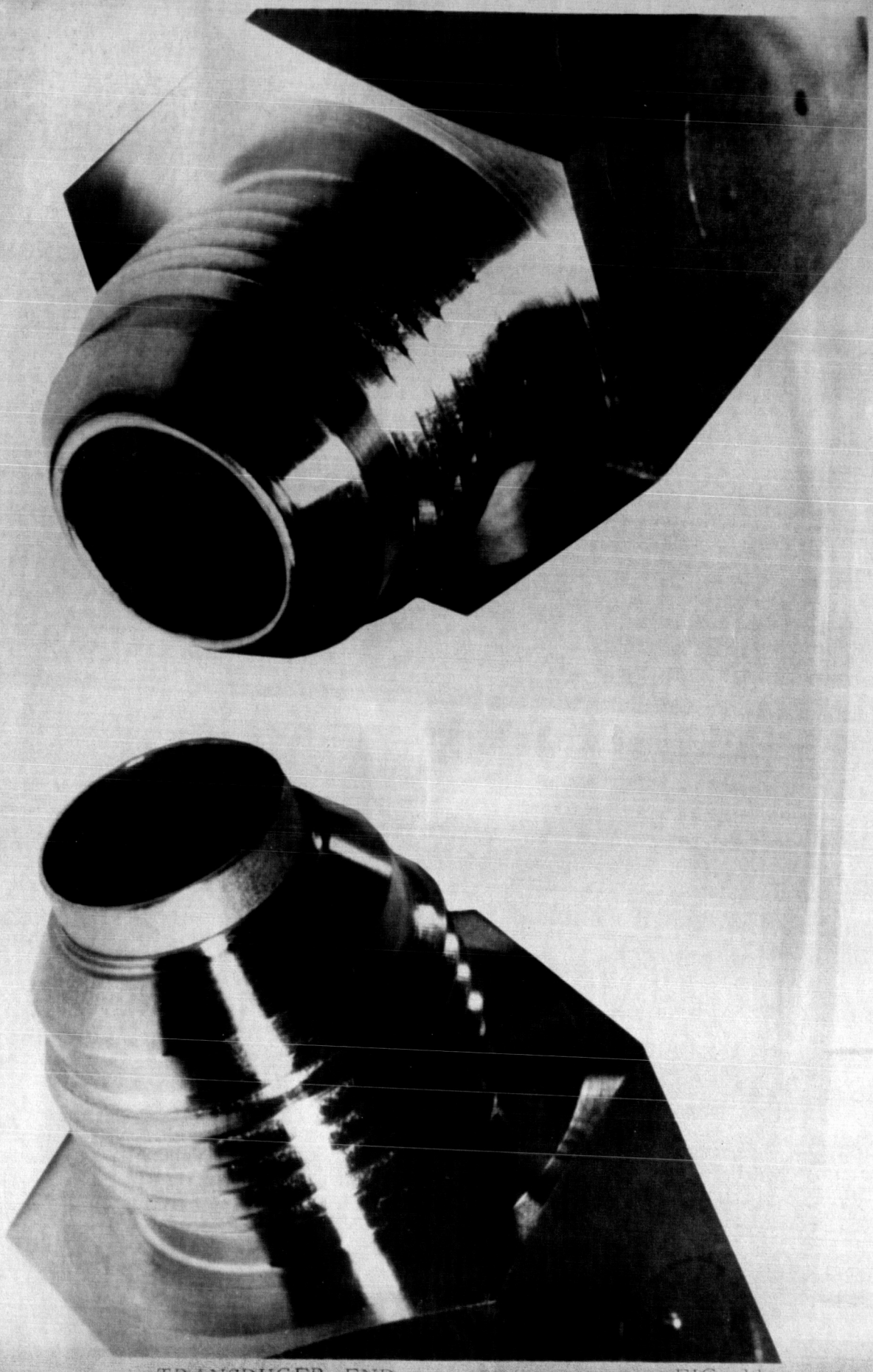

TRANSDUCER END

FIG. 1

shows a typical transducer end before and after applying the weld. The tubing end weldments complete the sealing of the transducers so that the propellant carrying portion is completely surrounded by a welded boundary of type 304 stainless steel.

The heater resistors and thermistors were then prepared for insertion in the transducers. The glass-sealed thermistor probes were cast into thermally conductive epoxy plugs which snugly fit the bore of the cross-stream tubes. The thermistors were then pressed into place and retained with a small spot of epoxy. The heater resistor was located in place and potted at both ends with silicone oil between the potted ends to enhance the thermal contact. This approach was used so that the transducers would be easily repairable. Flight type transducers will have both thermistors and resistors permanently bonded in place with epoxy. The thermistor and resistor leads were then resistance welded to nickel ribbons which were welded to an electrical connector. The electrical connector was a Physical Sciences type BLO2SM and had a type 304 stainless steel body and gold-plated stainless steel pins. The pins are individually insulated from the connector body by silico-ceramic inserts.

Figure 12 shows the electrical connector, a typical thermistor, the two sizes of cross-stream tubes and the connector mounting hole of the low range transducer. The electrical connector was welded in place using the tungsten-inert gas process.

Convection baffles were fabricated from 0.01" thick type 301 stainless steel sheet. They were pressed in place in the transducers delivered but will be spot-welded in flight versions of the transducers. Figure 13 is an end view of the low and high range transducers with the convection baffles in place. The cross-stream tubing assemblies and circumferential weldments holding the inner tubing assemblies to

TRANSDUCER COMPONENTS

PLDS TRANSDUCERS FIG. 13

the housings are also clearly visible. The transducer cases were each machined in two pieces from type 304 stainless hexagonal bar stock. The two pieces were provided with mating ring and groove joining surfaces and were heliarc welded together before finish machining.

B. Electronic System

The electronic system furnished with the transducers consists of a Propellant Leakage Detection System (PLDS), and a PLDS Test Unit. The PLDS contains the transducer signal amplifier, leakage threshold detector, leak alarm logic, and power supply circuitry. The PLDS Test Unit contains range switching, calibration and leak indication circuitry and was provided to facilitate testing of the PLDS.

Figure 14 is a block diagram of the PLDS. The transducer provides a bridge unbalance in response to flow. The bridge output signal is first amplified and then operates a threshold indication circuit consisting of a bi-stable amplifier. The resulting indication of leakage above the threshold level is connected to the logic circuitry which provides an output when the leak represents a malfunction condition. The logic required to perform this function was derived from the requirements for the low and high range systems as follows:

1. The alarm shall light during low range operation if the fuel or oxidizer flow is above the threshold, and the RCS is not energized.
2. The alarm shall light during high range operation if the fuel or oxidizer flow is above the threshold level and the RCS is not energized, or if either fuel or oxidizer flow is above the threshold level and the O/F ratio differs from 2.0 by more than 50%.

PLDS BLOCK DIAGRAM

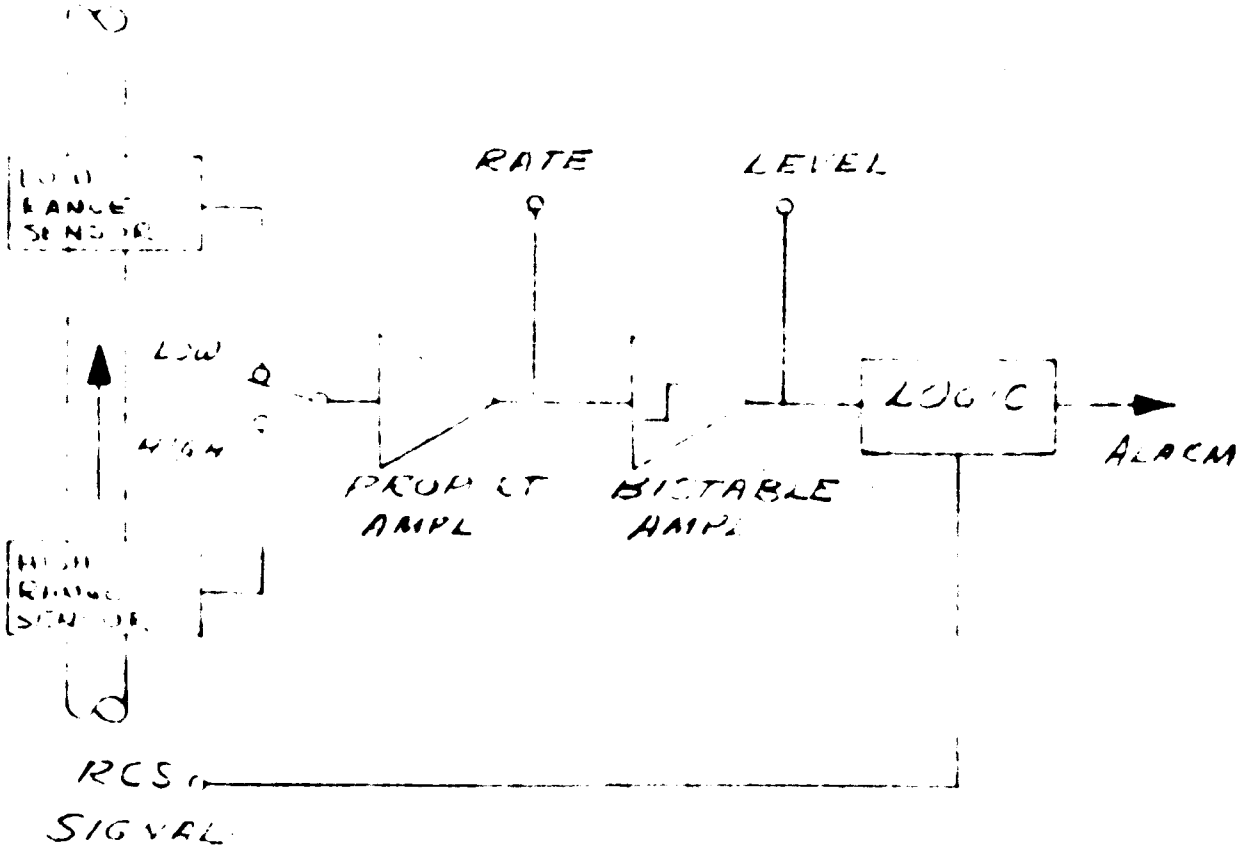

FIG. 14

These two requirements can be expressed as logical equations using the following notation:

A_l — Low range alarm lights

A_h — High range alarm lights

R — Reaction Control System is energized

L_o — Oxidizer flow above low threshold

L_f — Fuel flow above low threshold

H_o — Oxidizer flow above high threshold

H_f — Fuel flow above high threshold

Z — O/F ratio differs from 2.0 by more than 50%

The logical equations are:

$$A_l = \overline{R} \cdot (L_o + L_f)$$

$$A_h = \overline{R} \cdot (H_o + H_f) + (H_o + H_f) \cdot Z$$

Figure 15 shows the logic for the high range alarm signal in Veitch diagram form. (The low range logical equation is already in the simplest two-level form.) The maxterm mechanization of the high range logic is the simplest and is given by:

$$A_h = (\overline{R} + Z)\ (H_f + H_o)$$

The equation above indicates that the malfunction indication is desired if either the fuel or the oxidizer flow rate is above the high flow threshold and at the same time the RCS signal is absent or the utilization rates of fuel and oxidizer are in the wrong ratio.

Figure 16 is a block diagram of a PLDS which performs this function. The system delivered did not include separate fuel and oxidizer systems. The logical

VEITCH DIAGRAMS

HIGH RANGE LOGIC

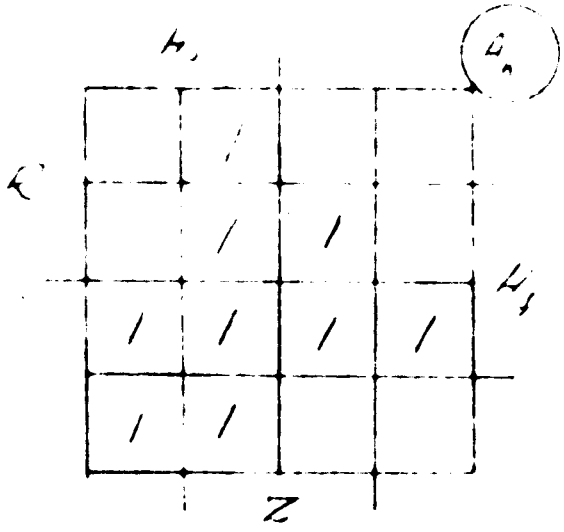

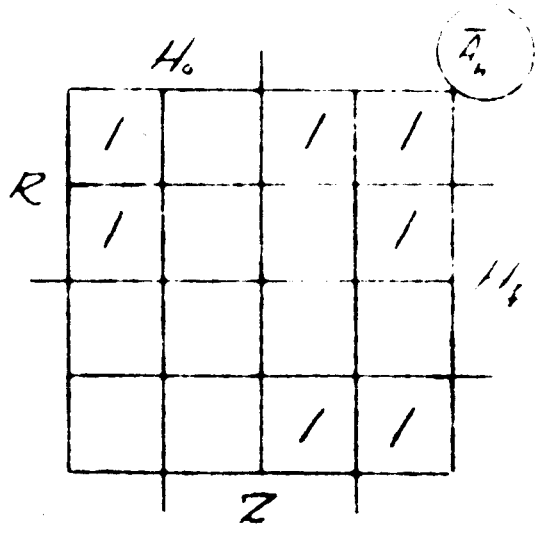

$$A_4 = \bar{R}H_0 + \bar{R}H_4 + H_0Z + H_4Z$$

$$\bar{A}_4 = R\bar{Z} + \bar{H}_4 \cdot \bar{H}_0$$

FIG. 15

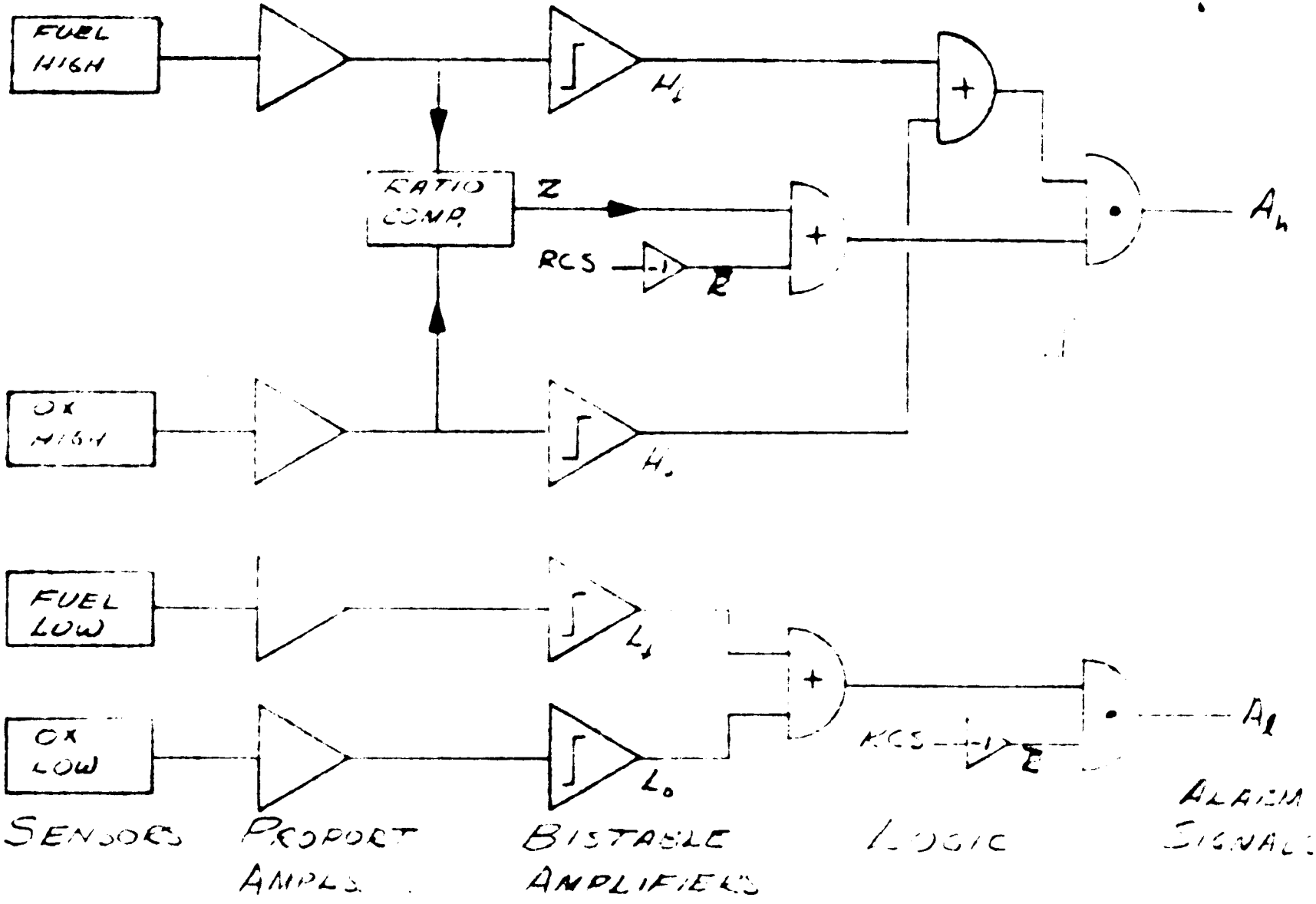

FIG 16

COMPLETE PLDS

equations were therefore simplified to:

$$A_l = \overline{R} \cdot L$$

$$A_h = \overline{R} \cdot H$$

Where L and H represent the condition of leakage above the low and high threshold levels, respectively.

The prototype PLDS used the same electronic system for both low and high range operation. The mode of operation was selected by a switch on the PLDS Checkout Unit. The high and low range logical equations were combined in the form:

$$A = \overline{R} \cdot T$$

Where A is the alarm indication and T represents flow rates above the threshold level.

The prototype PLDS was constructed using monolithic integrated silicon amplifiers and logic elements. Figure 17 is a photograph showing the components of the PLDS mounted on the epoxy-glass circuit board in the aluminum outer case. The electrical connections on the prototype PLDS were made by point-to-point wiring on the reverse side of the circuit board.

The metal film resistors and monolithic silicon electronic devices used in the PLDS are similar to those currently in use on the Apollo and LEM Programs and were selected to provide the reliability and environmental resistance needed for spacecraft electronic equipment.

Figures 18 through 20 are schematic diagrams of the PLDS Test Unit. The PLDS Test Unit contains circuitry to select either the high or low range transducer for input to the PLDS, a calibration circuit for connecting resistors across the

ELECTRONIC SYSTEM

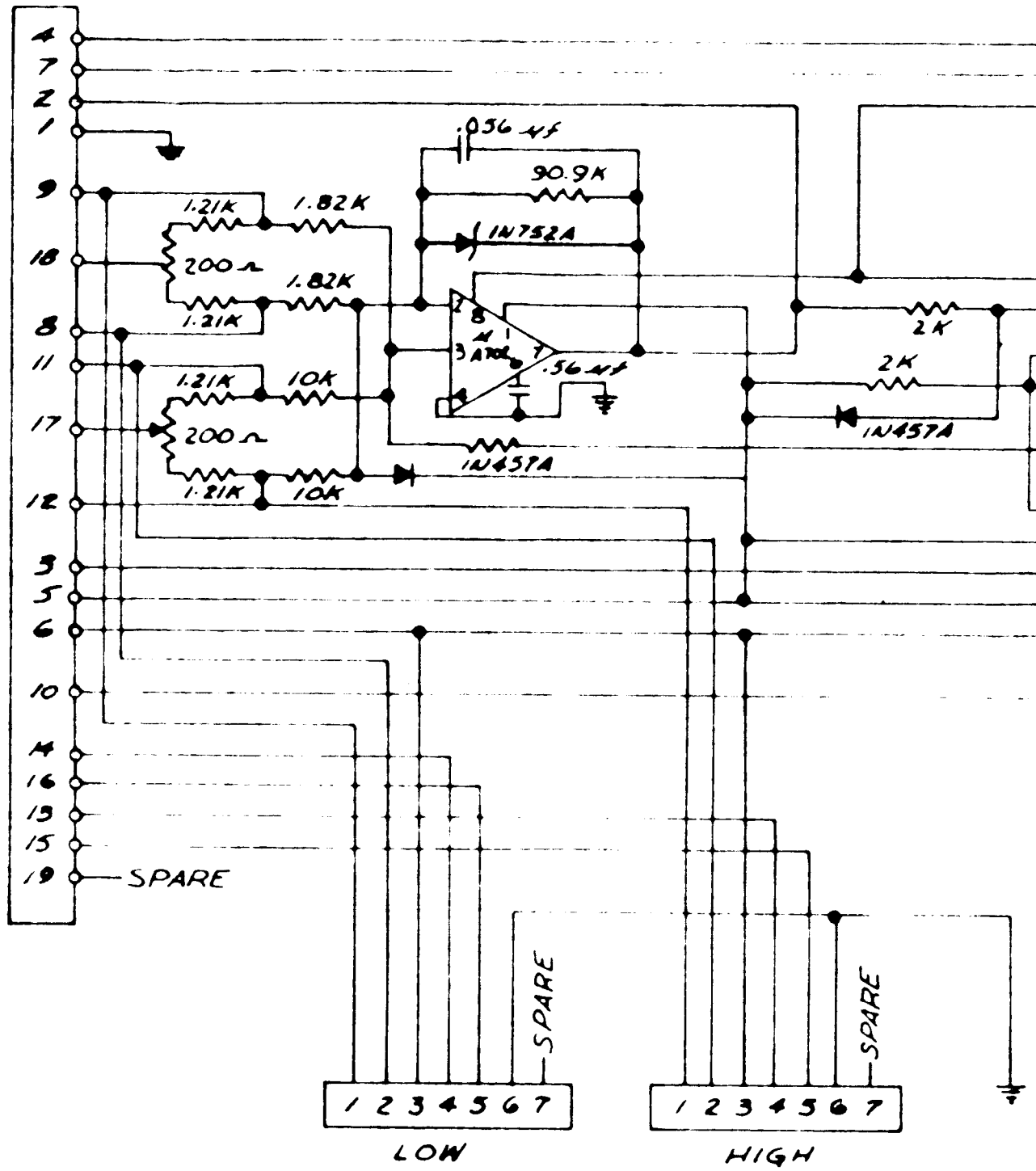

PROPELLENT LEAKAGE DETECTION SYSTEM

FIG. 18

Spacelabs, Inc.

SIGNAL VALVE INPUT (+28V)
+28V
GND

1N4001

Rc1
Rc2
"CALIBRATE"

NC
C
NO

680Ω 1W

#327 "LEAK"
100Ω
2N2270
+28V "PWR"
100Ω
2.7K
1.5K

LO
HI
RANGE

4.7K
4.7K
+28V
"RATE"

TEST POINTS

+18V
"LEVEL"
+6V
"ALARM"
GND

PLDS TEST UNIT

Spacelabs, Inc.

FIG. 19

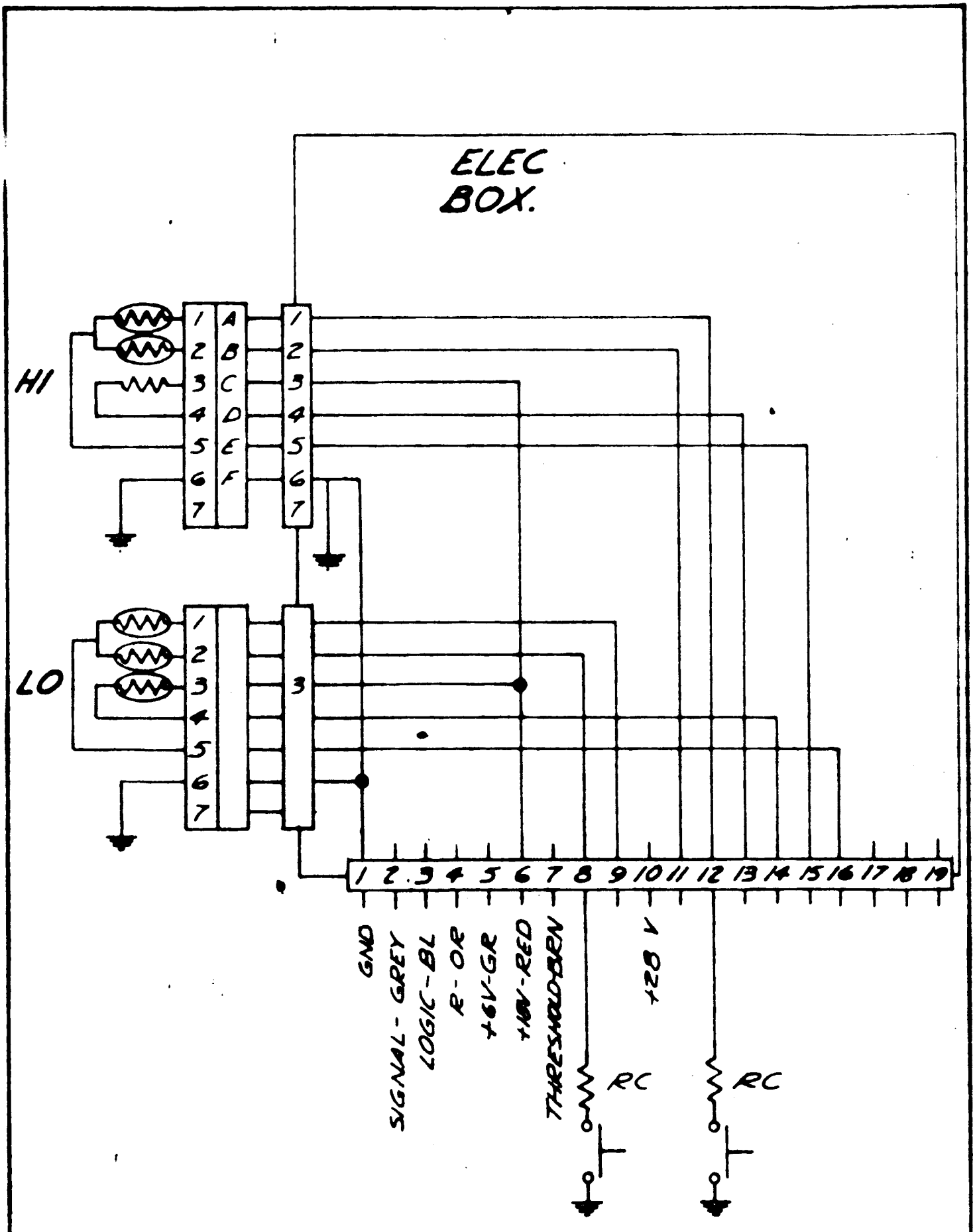
ELEC
BOX.
HI
LO
1 A
2 B
3 C
4 D
5 E
6 F
7
1 2 3 4 5 6 7 8 9 10 11 12 13 14 15 16 17 18 19
GND
SIGNAL - GREY
LOGIC - BL
R - OR
+6V - GR
+18V - RED
THRESHOLD - GRN
+28 V
RC
RC

FIG. 20

thermistor sensing elements for calibration, a power indicator light, a number of test points for monitoring the performance of the PLDS components and a leak alarm indicator and indicator lamp driving circuitry.

The test points make it possible to monitor the 28 volt supply voltage (after the protective diode), the 6 and 18 volt internal PLDS power supply voltages and the output signals of the proportional amplifier, the bi-stable amplifier, and the logic circuitry. The proportional amplifier output provides an analog measurement of flow rate for later use in O/F monitoring and propellant management schemes.

C. System Characteristics

The prototype PLDS delivered consisted of a high range transducer, a low range transducer, a PLDS electronic system and a PLDS checkout unit. The high and low range transducers could be contained in a single package in future systems but were separated for manufacturing and testing reasons in this development program. The low range and high range transducers weighed 454 and 478 grams, respectively, and the electronic system weighed 346 grams. All these weights could be considerably reduced without sacrificing performance in a flight unit.

The prototype Propellant Leakage Detection System would be capable of operating over all applicable Apollo environmental conditions after potting.

Sensor Design

The prototype Propellant Leakage Detection System fabricated under this program embodies solutions to problems which seemed very difficult at the start of the program. The welded stainless steel construction technique used for the sensors provides complete protection of the sensing

elements from the propellants. Sensors constructed in this manner can be used for a wide range of applications to provide flow measurements and leakage detection for corrosive fluids. The rugged simplicity of the design makes it suitable for incorporation in space vehicle propellant systems without compromising system reliability. The sensor could be installed with conventional fittings or could be designed to be welded in place in the propellant system plumbing.

The sensor is designed to provide a high level of environmental resistance. The structural elements of the transducers have high natural frequencies and the joints between the cross-stream tubes and the main flow tube are designed to provide frictional damping to minimize resonant amplification. This is a design technique of proven value and has been used to provide structural damping in turbojet fuel injection spray bars. The prototype sensors delivered at the program end, with the addition of potting compound to hold the internal wires in place, should easily endure the expected vibration levels.

The thermistors used in the sensors were Victory Engineering Co. type 32A129. They are of the bead-in-glass-probe type construction. The manufacturer claims that similar thermistors have compiled an aggregate of 10^8 sensor hours on the Titan I Program without a failure.

Electronic System Reliability

The electronic system is designed using high reliability silicon diodes, transistors and monolithic integrated silicon amplifiers and logic circuits. The resistors used were metal film types that are currently also being used on the Apollo and Gemini Programs. Table I summarizes the

ESTIMATED RELIABILITY FOR PLDS COMPONENTS

Part Type	Failure Rate Source	Failure Rate %/1000 Hours	Number Used	Total F. R. %/1000 Hours
Resistors				
Carbon Composition	Mil-HDBK-217	0.001	7	0.007
Metal Film	ADS38101/1A	0.0005	20	0.010
Variable	Estimated	0.004	2	0.008
Capacitors				
Ceramic	ADS38102/12	0.006	4	0.024
Tantalum Electric	ADS31802/4	0.004	2	0.008
Diodes				
Zener	ADS38103/110	0.0250	2	0.050
Silicon Computer	ADS38103/121	0.0025	6	0.015
Transistors	ADS38103/310	0.002	4	0.008
Integrated Circuits				
Logic	Fairchild Tests	0.003	1	0.003
Amplifier	Estimated	0.040	2	0.080
Connectors	Estimated	0.015	5	0.075
Thermistors	OTS-PB-181080	0.03	4	0.120
			TOTAL	0.408

TABLE I

estimated reliability of the components of the PLDS. The estimated failure rate for the prototype system delivered is 0.408%/1000 hours which is equivalent to a MTBF of 245,000 hours. The addition of a separate system for a second propellant and the extra circuitry for O/F ratio evaluation might reduce this MTBF to 100,000 hours.

The thermistors are inherently radiation-resistant and should be reliable and stable in spite of exposure to Van Allen belt levels of radiation.

Temperature Compensation

The low range transducer is designed so that it will indicate zero leakage correctly independent of fluid temperature, provided the two thermistors are well matched. During ground testing there will be a loss of sensitivity to low flows due to the influence of free convection. Since this change in sensitivity disappears during actual service in a zero-G environment, it is not desirable to provide temperature compensation for it. The temperature independence of the low flow zero indication makes ground checkout practical and therefore greatly enhances the system utility.

The high range transducer tends to provide the same signal at very high flow rates independent of fluid temperature. This is true because the heater temperature is allowed to approach fluid temperature at high flow rates. As this happens, the two thermistors also approach the fluid temperature and the transducer output becomes independent of temperature except for thermal mismatch between the thermistors. This thermal mismatch will probably be larger in the high flow transducer delivered because only one set of factory matched thermistors was available and

this was installed in the low range transducer. The thermistors in the high range transducer were selected from a number of thermistors on hand to provide the best match in room temperature resistance.

At low flow rates, the changes in fluid properties cause changes in heat transfer and therefore in transducer output signal. These changes could be compensated by adding an extra thermistor in the same tube with the upstream sensor. This thermistor would be used to provide an adjustment of system sensitivity for temperature. Temperature compensation was not provided in the prototype system because of the lack of propellant facilities needed to determine the proper compensation and because the uncompensated performance of the transducers was quite good.

Power Consumption

The power required by the prototype PLDS was approximately 1.6 watts. This included the 0.5 watts supplied to the heater and the power consumed by the electronics. The same power consumption applies to both low and high flow warning systems. When operated with the PLDS checkout unit, the power consumption is higher (about 3 watts) because of the pilot light, alarm indicator and range changing circuitry in the checkout unit. The 1.6 watt figure is the actual power consumption of the PLDS. This could be reduced considerably through additional work on the circuitry, such as operating the amplifiers at reduced voltage, but this was not done in the prototype system.

V EVALUATION TESTS

After fabrication of the prototype system, a set of evaluation tests was conducted to demonstrate that the technical objectives of the program had been met.

The evaluation tests included investigation of the effects of temperature and position on the performance of the system and determination of the system response and warm up times. Figure 21 is a schematic of the evaluation test apparatus. Figure 22 shows the system under test.

Before evaluating the low and high range systems, tests were conducted which proved that the power supply voltage could be varied from 24 to 32 volts without appreciably affecting system performance.

Low Flow System Tests

The low range transducer was installed with its flow axis horizontal and with its electrical connector in a horizontal plane. This places the convection baffles in the most effective orientation. Data were taken of flow rate versus output voltage (measured between "Rate" and "Ground") for 55°F and 90°F water temperatures. These data are presented in Figure 23. It can be seen that the zero leakage indication is insensitive to temperature because of the symmetrical design of the transducer. The threshold level (at which the "alarm" light goes on) is also indicated on the figure.

The alarm level varies from 25 to 50 cc/hour over the temperature range. This variation is due to the free convection effects discussed previously and will not exist during zero-G operations. The test results show that the sensitivity goals for the low range system have been met.

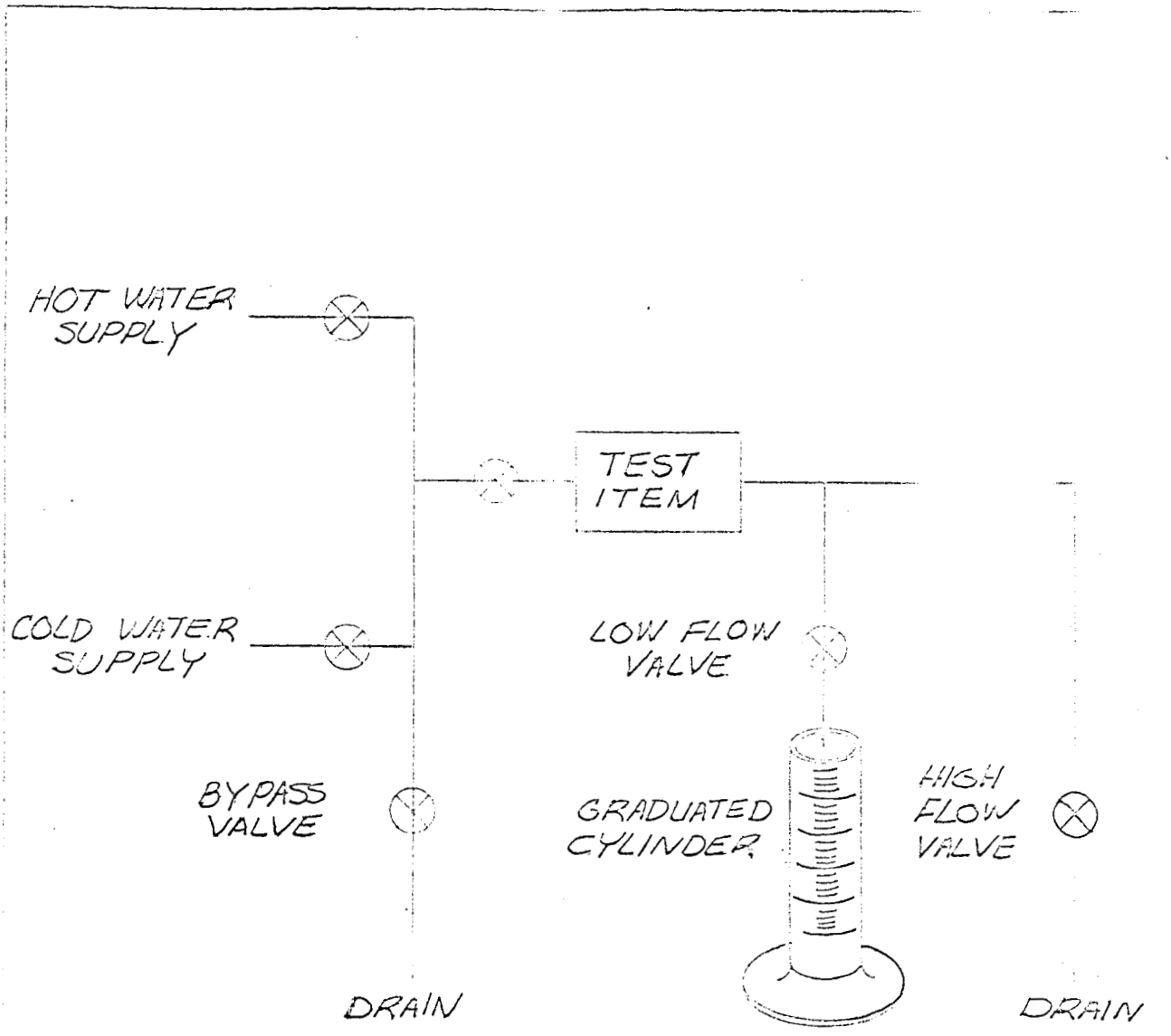

TEST FACILITY SCHEMATIC

FIG. 21

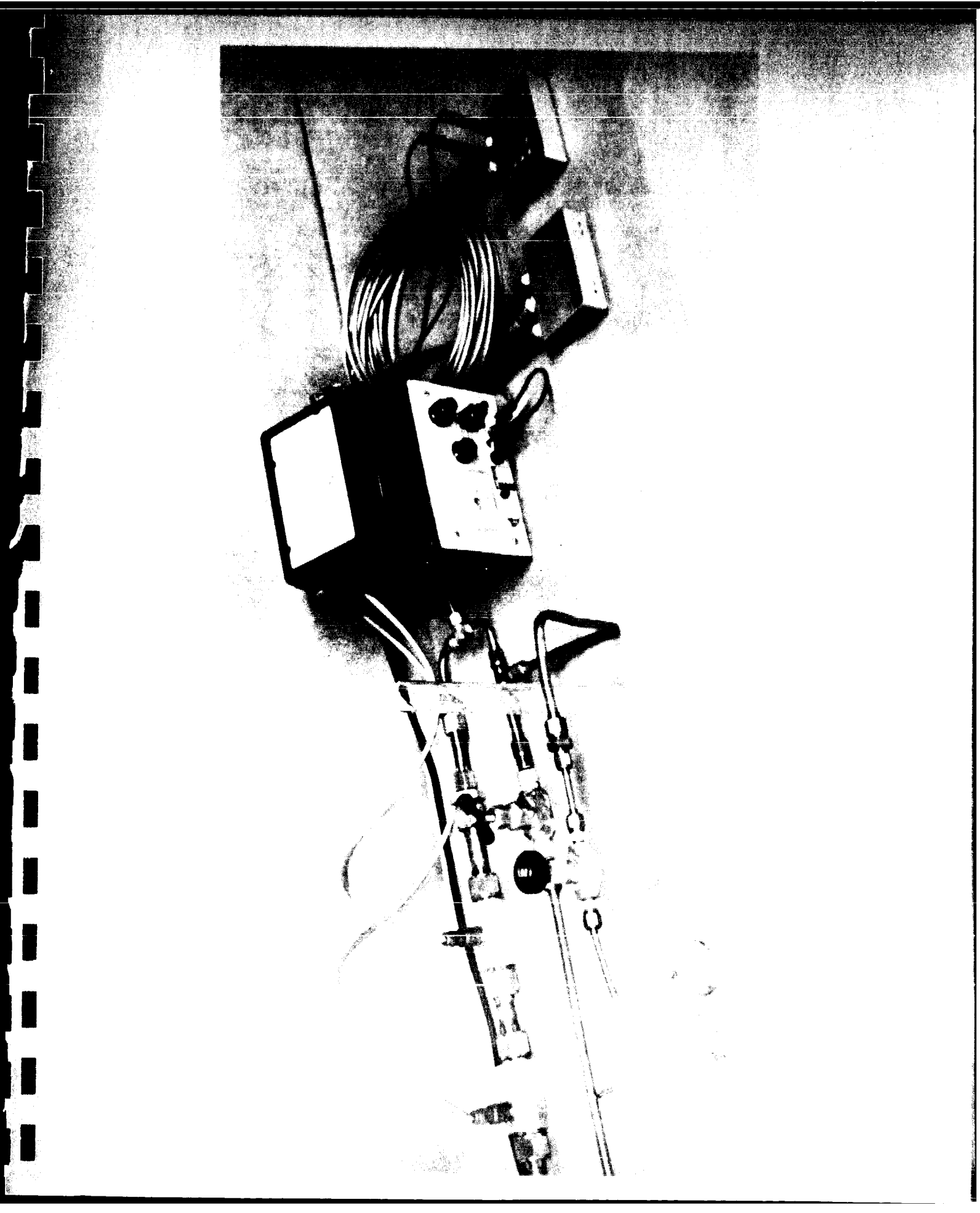

Figure 23 also shows the output signal of the low range system at higher flow rates. It can be seen that the signal stays above the alarm level until the flow rate reaches 100,000 cc/hour. This is considerably beyond the required 1800 cc/hour upper limit for the low range system.

In Figure 24, the flow rate equivalent to the signal obtained by tilting the flow axis of the transducer is plotted against angle of tilt. These data provide an indication of leveling requirements during ground testing. It is seen that the transducer should be leveled within 0.1° of horizontal for very critical work. Leveling "by eye" is adequate for most testing.

The response time of the low range system was determined by setting up a leak rate of 40 cc/hour and then turning the electrical power on. Figure 25 shows the resulting output voltage plotted against time. The alarm goes on about 0.7 min after the system is energized. This is well within the 10 minute requirement for response time.

A leak rate of 800 cc/hour was set up and then suddenly removed to determine the time required to reach a zero leak indication after leak removal. The output voltage is plotted against time in Figure 26 which shows that the zero leak indication is reached within 0.5 minutes.

High Flow System Tests

The high range sensor is designed so that the thermistors operate at different temperatures at zero flow. When the high range system is first energized, they are at the same temperature. The variation of system output with time after first applying the power is shown in Figure 27. It can be seen that the alarm is on for the first 0.1 minutes after system

LOW RANGE PERFORMANCE

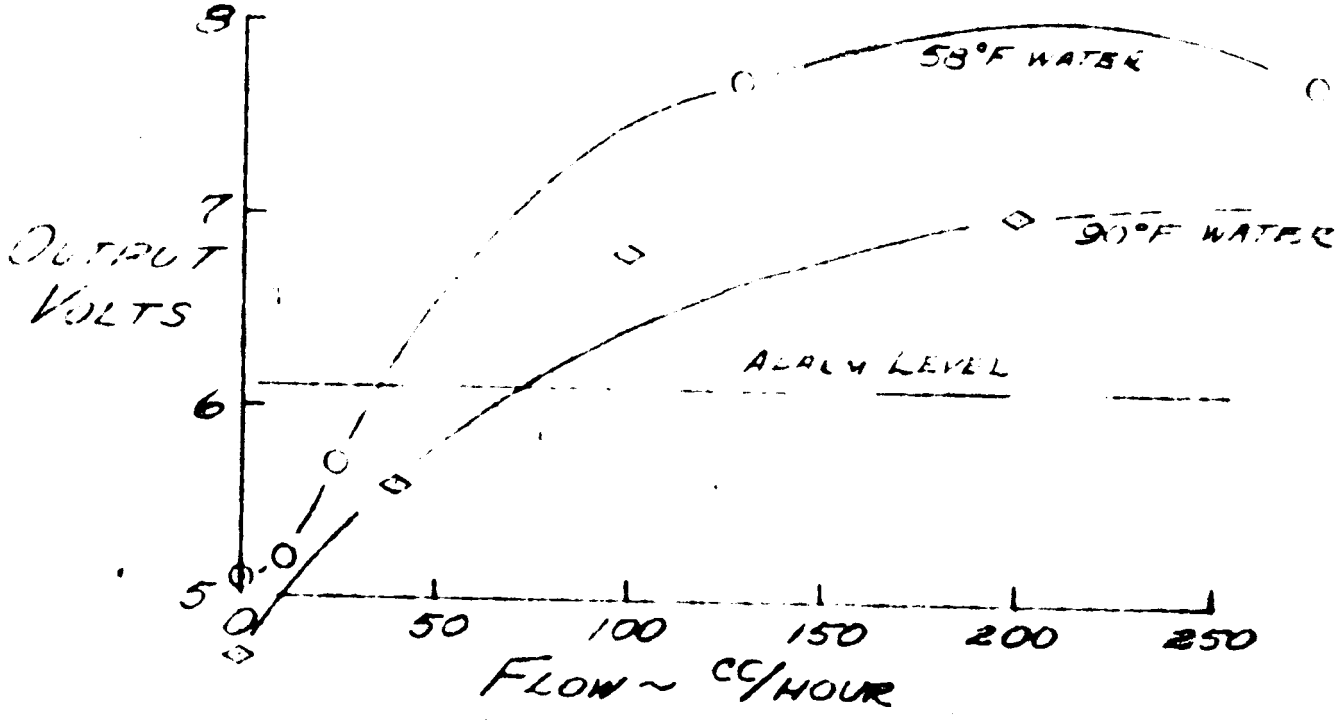

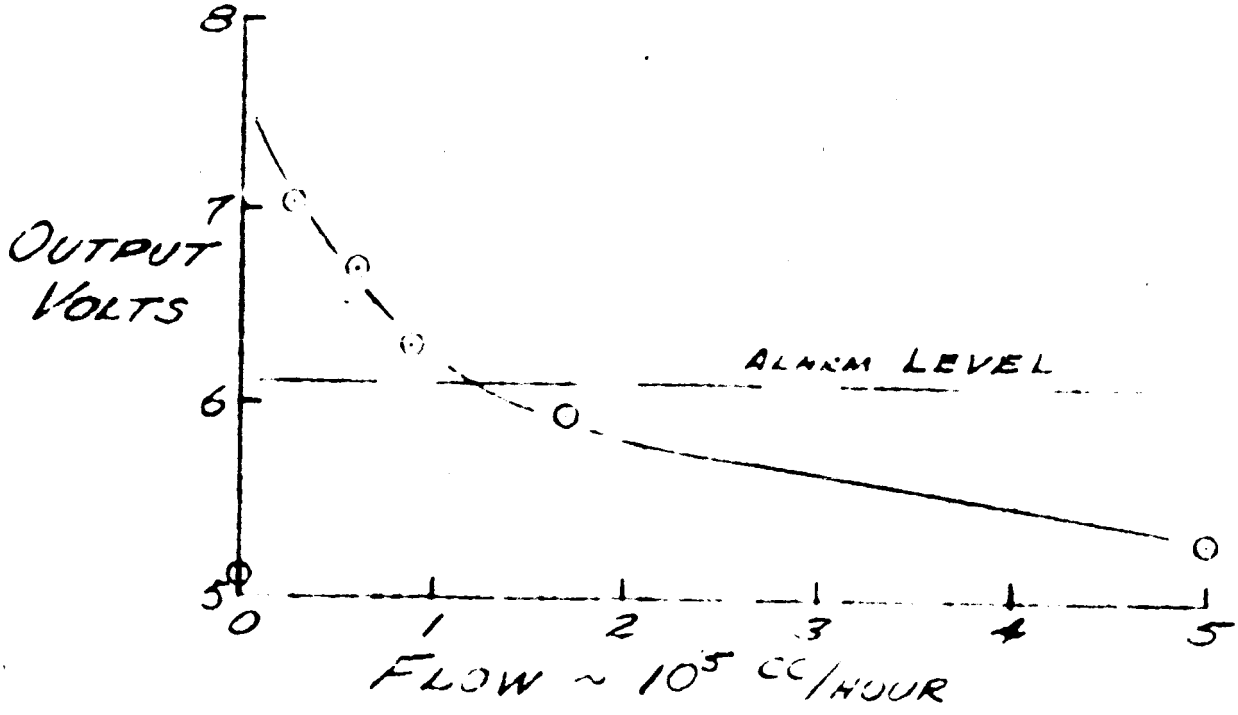

FIG. 23

LOW RANGE ATTITUDE SENSITIVITY

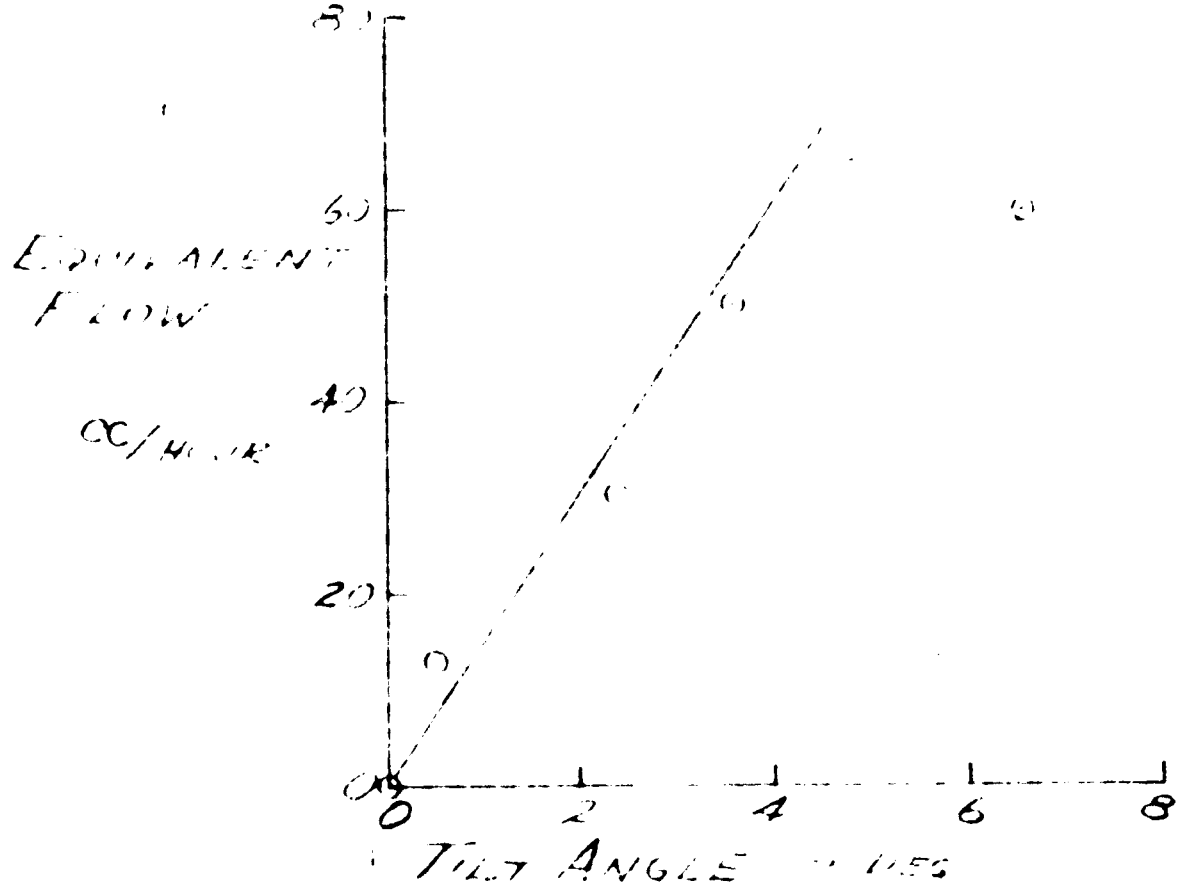

FIG 24

LOW RANGE
ALARM

LEAK RATE = 40 cc/HOUR

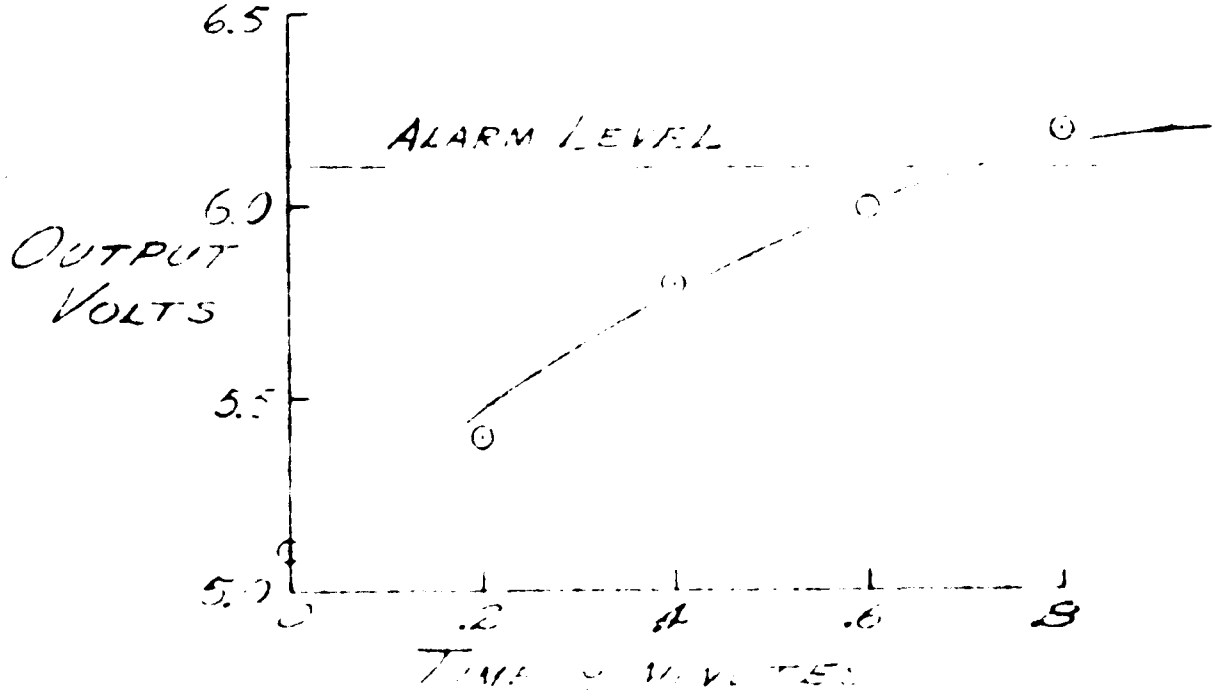

FIG 25

LOW RANGE RECOVERY

(FLOW OF 300 c/min JUST REMOVED)

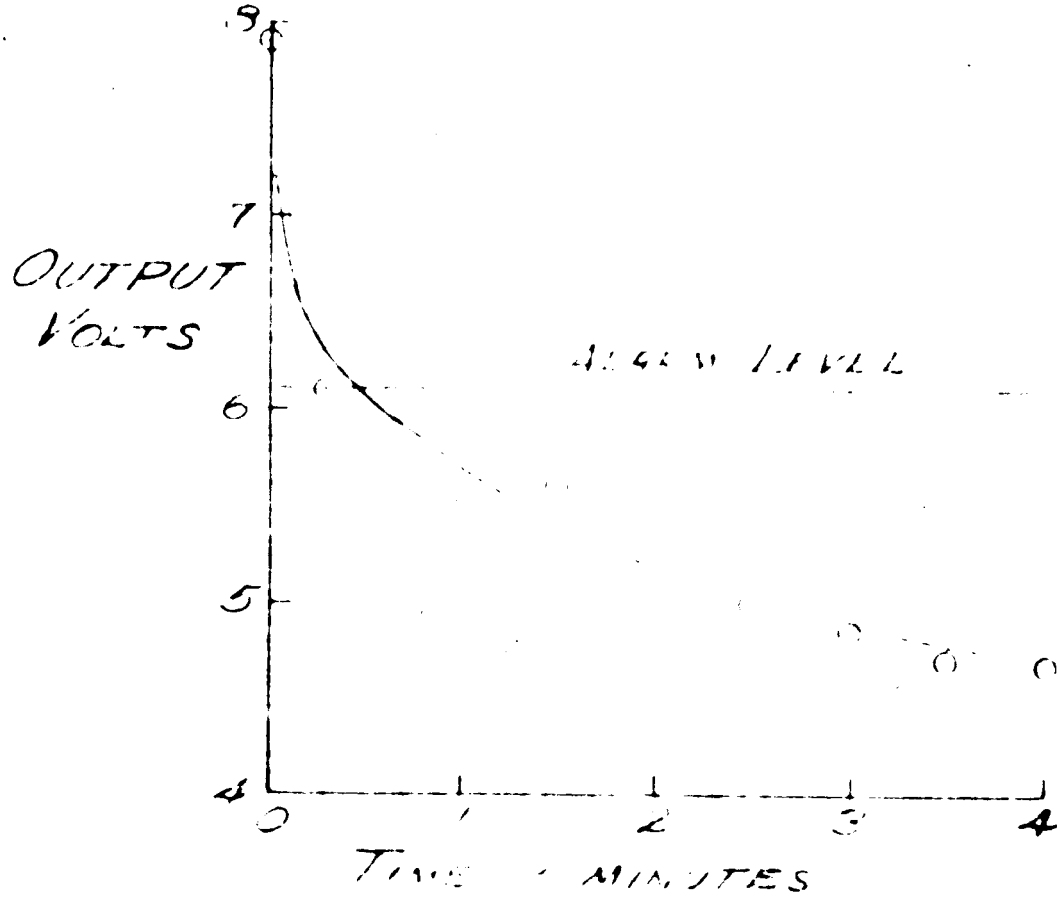

Fig 36

HIGH RANGE WARMUP

(ZERO FLOW)

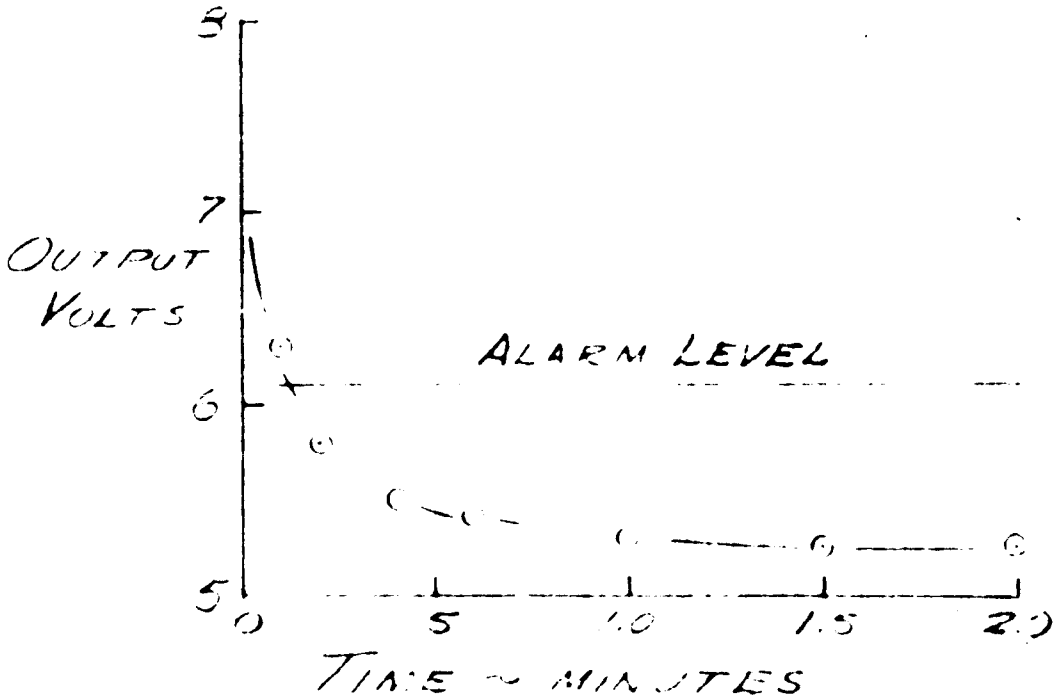

FIG. 27

turn-on. The system will indicate zero leakage after 0.1 minutes and is fully warmed up after two minutes.

Data were taken of the output of the high range system for both 59° and 90° water temperatures. The data are presented in Figure 28.

The data show that satisfactory leak indication can be obtained over the temperature range without temperature compensation. Figure 28 also shows the output of the high range system at water flow levels equivalent to the full RCS flow rates on a heat transfer basis (see Appendix C). The data show the system's ability to respond to high flow rates in spite of the fact that the passive heater system trades low power consumption for high flow sensitivity. The construction of an O/F monitoring system does appear feasible if both oxidizer and fuel systems were built.

Figure 29 shows the flow error due to rotation of the flow axis from a horizontal to a vertical position. It can be seen that the error never exceeds 600 cc/hour even with the flow axis vertical. It does appear desirable to orient the high range transducer axis perpendicular to gravity and acceleration directions to minimize calibration changes at low flow rates. At higher flow rates there will be no noticeable acceleration effects.

HIGH RANGE PERFORMANCE

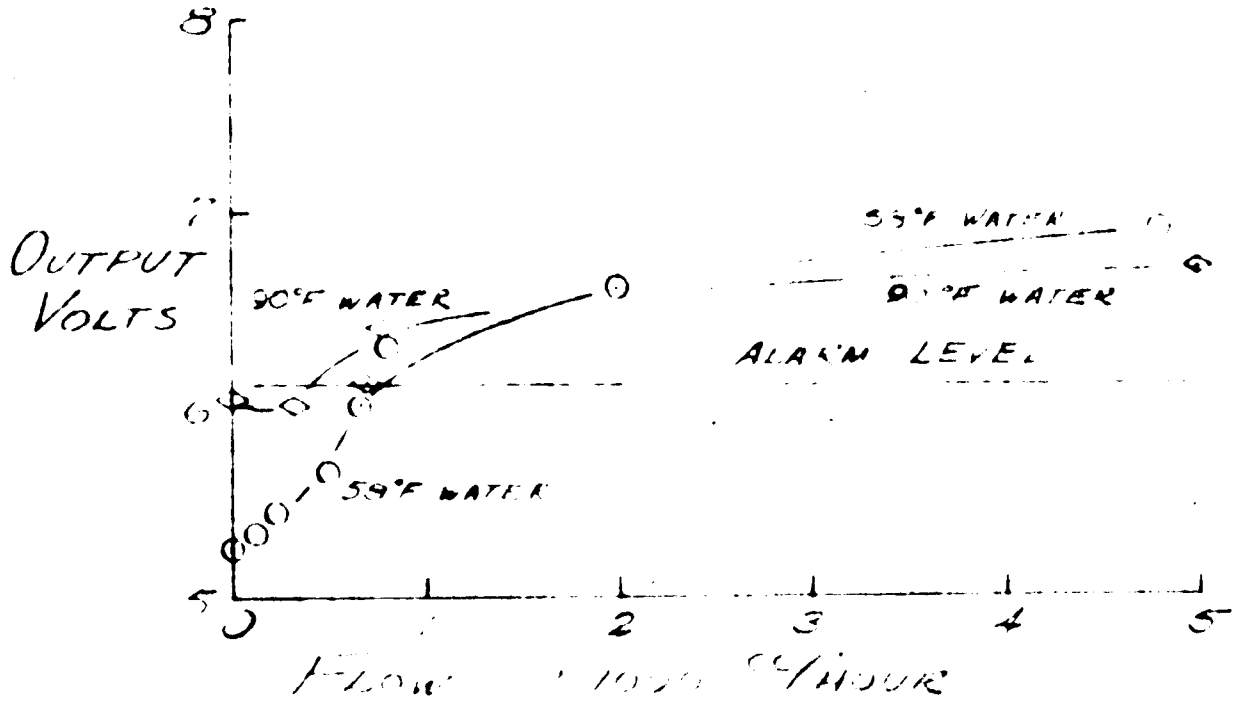

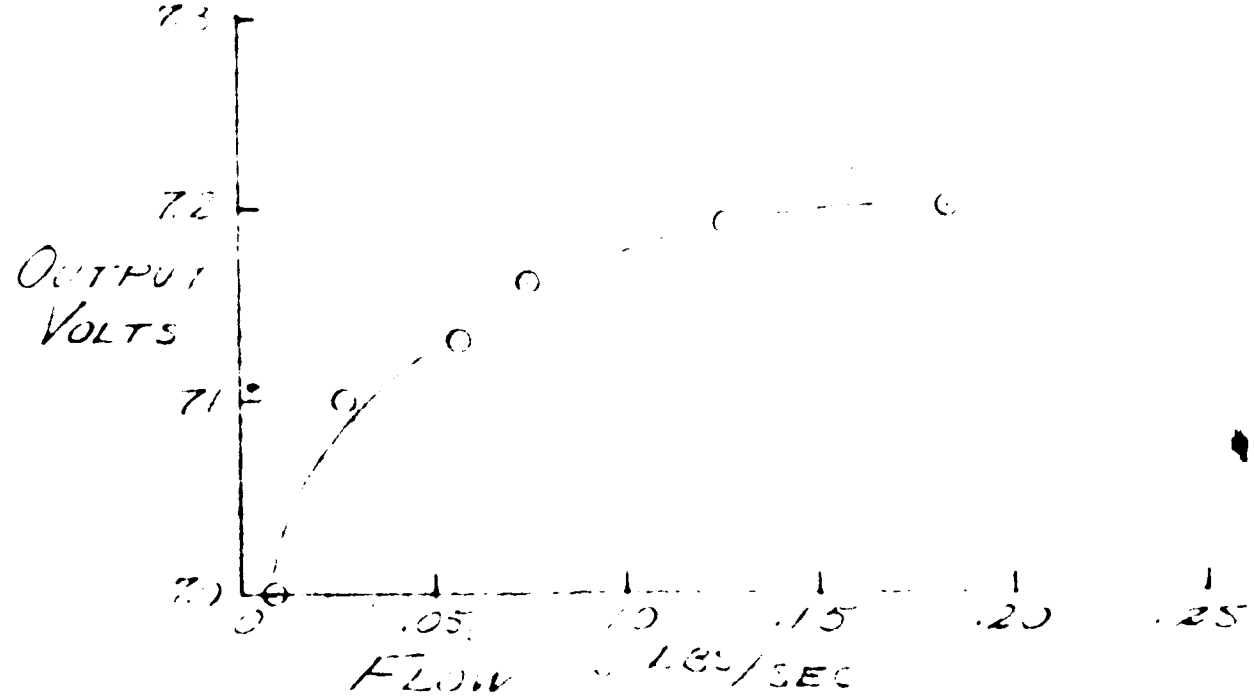

FIG 28

HIGH RANGE
ATTITUDE SENSITIVITY

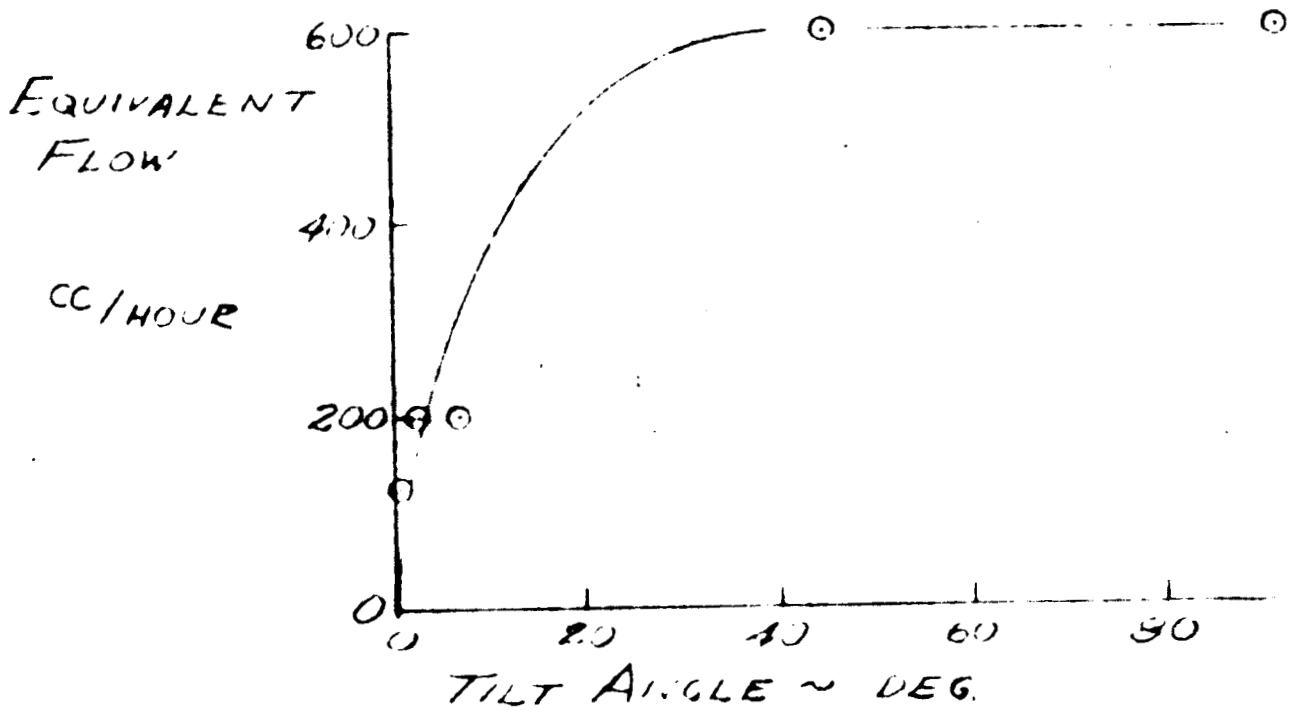

FIG. 29

VI CONCLUSIONS AND RECOMMENDATIONS

The program objectives were satisfied and the hardware was delivered on schedule. The technology embodied in the prototype Propellant Leakage Detection System provides a good basis for design of production systems. The major technical problems associated with meeting the specifications have been solved. The measurement techniques developed in the course of the program cover a much wider range of applications than originally envisioned. Some specific significant observations are summarized below.

1. The program has produced a number of simple, completely propellant compatible transducer design configurations which are suitable for incorporation in space vehicles without compromising the vehicle reliability. These include the design of the low and high flow sensors, the dual range sensor in a single housing and the obstructionless high range sensor with external windings. All of these designs are fully propellant-compatible and have no static or dynamic seals.

2. The transducer configurations developed can be used to make flow measurements in many corrosive liquids and gases such as fluorine, flox and other fluids for which no satisfactory flow measurement technique presently exists.

3. The circuitry techniques used in the electronic system will provide good performance and reliability in flight vehicle environments. The proportional amplifier, bi-stable amplifier, logic and power supply circuits may be combined in a variety of ways to provide different functions such as O/F monitoring, flow rate monitoring, leak measurement, leak threshold detection, etc.

4. The high flow sensor can be operated with the heater temperature held constant by a servo system built around the same type of circuitry used in the delivered system. Such a system will consume more power (but less than 5 watts per transducer) and will provide time constants of the order of 100 milliseconds. It would be more sensitive at high flow rates because the heater temperature would not be allowed to fall.

5. Sufficient knowledge has been generated to allow design and production of flight-type Propellant Leakage Detection Systems.

6. The measurement techniques developed provide good measurements in a range of low liquid flow rates difficult to instrument with conventional transducers such as turbine meters.

APPENDIX A

REVIEW OF THE STATEMENT OF WORK

This Appendix relates the accomplishments of the program to the specific requirements enumerated in the Statement of Work. The characteristics of the prototype PLDS fabricated under this program are compared with the Work Statement goals.

I Scope

The Propellant Leakage Detection System desired is a lightweight compact system achieving reliability through simplicity and capable of providing detection of both extremely small leaks and of unusually high propellant utilization rates. The system delivered demonstrated the feasibility of accomplishing these goals.

II System Requirements

A. Integration Requirements

1. The PLDS can be integrated into present expulsion systems without major alterations to essential components of RCS, PLDS or PQGS (Propellant Quantity Gaging System).

2. The PLDS could be designed to function in conjunction with, or as part of, the PQGS.

3. Propellants - The PLDS transducers delivered are designed for use with nitrogen tetroxide and hydrazine family fuels.

4. Compatibility - All portions of the PLDS that will be exposed to propellants are constructed of 300 series stainless steels and offer long-term chemical resistance to these propellants.

The high flow warning system has a first order time constant of 0.6 seconds at full flow. If a large leak suddenly occurs, the

alarm will be given within a few milliseconds which is well below the 200 milliseconds required.

5. O/F Ratio - The O/F ratio of 2.0 is equivalent to a heat transfer ratio of about 1.3, therefore, the same transducer sizing can be used for both fuel and oxidizer.

6. Operating Pressure - The operating pressure range of 100 to 300 psi will cause no problems.

7. Operating Temperature - The system will not be damaged by temperatures ranging from 0 to 140°F. The system will operate satisfactorily over the 20°F to 85°F range of temperatures expected during a normal duty cycle.

8. Line-Size - The transducers delivered had standard -12 end fittings designed for testing with standard 3/4-inch line sizes. The design is easily adaptable to installation in 3/4-inch and 5/8-inch RCS plumbing by using fittings or by welding.

9. Flow Rates - The transducers are designed to cover the flow rates expected during RCS operation.

10. Fail-Safe - The PLDS is designed so that no failure in the PLDS shall compromise the reliability of the RCS. The transducer reliability can be as good as the reliability of the line length it replaces.

11. Component Packaging - The components of the PLDS are separated into transducers (for installation in the propellant flow system) and electronics for signal conditioning. The transducers are propellant-compatible and the electronic system can be designed for switching between many transducers.

B. RCS Failure Modes to be Detected

The PLDS developed will detect both the small leaks associated with valves improperly seating and the large leaks associated with valves failing open and with line failures.

C. Design Specifications

1. Pressure Drop - The pressure drop through the PLDS transducers can be less than 1% of the operating pressure.

2. Pressure and Temperature Variations - The PLDS is inherently insensitive to pressure. The low flow warning system provides a zero leak indication which is inherently unaffected by temperature. Temperature compensation can easily be provided if desired in the high flow warning system.

3. Duty Cycle - The low flow detection system can detect leaks in the range from 20 cc/hour and above 15,000 cc/hour. This range considerably exceeds the Work Statement requirements.

The high flow leakage warning system covers the flow range specified and can be designed for O/F ratio detection using the transducers and circuit techniques developed.

4. Response Time - The response time of the low flow detection system is of the order of one minute from system initiation to warning. This is ten times faster than the 10 minute requirement.

The high flow warning system has a first order time constant of 0.6 seconds at full flow. If a large leak suddenly occurs, the alarm will be given within a few milliseconds which is well below the 200 milliseconds required for 60 cc of leakage.

5. Spacecraft Disturbances - The spacecraft disturbances expected do not contain a directed acceleration component of appreciable duration and will not disturb the operation of the low flow detection system.

6. Location - The planned location of the leak sensing package appears satisfactory.

7. Power Requirements - The prototype PLDS required 28 volts at about 1.6 watts for either the low or high range system. A dual fuel and oxidizer system would therefore consume 3.2 watts. Although this is less than the 5 watts allowed for the high range system and certainly less than the 25 watts allowed for the low range system, the power consumption could be reduced still further if desired.

8. Reliability - The prototype system has an estimated MTBF of 245,000 hours and is fail-safe with respect to the RCS.

9. Weight and Volume - The prototype transducer weights were about 460 grams. This could easily be cut in half in a production version. The electronic system weighed 346 grams and occupied about 12 cubic inches. The size of the electronics could be greatly reduced by employing the welded cordwood construction technique used for other Spacelabs flight electronic hardware.

10. Component Development - The components vital to system operation have been developed.

11. Radiation - The PLDS should function properly in the presence of normal interplanetary radiation levels.

12. Propellant Leakage - The transducer body and the inner tubing assembly both form separate redundant welded enclosures and prevent propellant leakage over the range of temperatures and pressures expected.

13. Acceleration - The high flow warning system will perform in a 6 G environment and will withstand 8.5 G's.

14. Shock - The system will withstand the applicable shock loading after potting.

15. Vibration - The system will withstand the vibration environment specified after potting.

III Specific Requirements

A. A prototype PLDS has been developed and tested. It provides the

specified sensitivity over the range of environments, integration requirements and design specifications outlined in the Statement of Work.

1. Prototype Leak Detector Development - The leak detection devices and control electronics have been designed and fabricated in finished breadboard form.

2. Leak Alarm Subsystem Development - The PLDS checkout unit provides leak alarm displays and is suitable for use in demonstration tests.

3. Demonstration Tests and Delivery - Evaluation tests have been conducted on the prototype PLDS and have proven the capabilities of low and high leak detection and the feasibility of providing O/F ratio out-of-limit indication. The equipment comprising the prototype PLDS was delivered on schedule.

B. The technical problems of meeting PLDS requirements have been solved.

C. This report completes the reporting requirement.

D. Sufficient knowledge has been generated to enable the design and fabrication of a full-scale optimized system under a later program.

APPENDIX B

EXPERIMENTAL PROGRAM

EXPERIMENTAL PROGRAM

An extensive experimental program was conducted to help identify problem areas and to measure the value of various approaches to the leak detection problem. Early tests of transducers using the variation of heat transfer coefficient as a measurement of flow rate indicated serious problems at the low end of the flow range. These problems were associated with the fluid velocities due to free convection being much higher than the flow velocities being measured. Conventional electrothermal flowmeters, therefore, do not exhibit adequate sensitivity to detect leak rates of 25 cc/hour and are extremely position sensitive. Figure 30 is an example of the low flow performance of a conventional electrothermal flowmeter design using a circumferential heater-sensor winding. It can be seen that the convective effects make the flowmeter unusable at very low flow rates. The output characteristic actually goes down for increasing flow between 0 and 400 cc/hour when the meter is oriented with the flow axis horizontal.

The problems encountered during these early tests pointed out a need for a different approach to the low leakage measurement problem. After analysis of the data and heat transfer relationships, it was decided to try a new low flow measurement technique. The method selected measures the temperature differential between two points located equal distances from a heated element. The measurement points are symmetrically located upstream and downstream from the heated element. The symmetry provides a zero signal at zero flow, independent of the influences of gravity and other disturbances.

The first thermal differential transducer tested consisted of two bead thermistors located in a $\frac{1}{2}$ inch outer diameter copper tube and spaced about $\frac{1}{2}$ inch apart.

CONVENTIONAL METER ATTITUDE SENSITIVITY

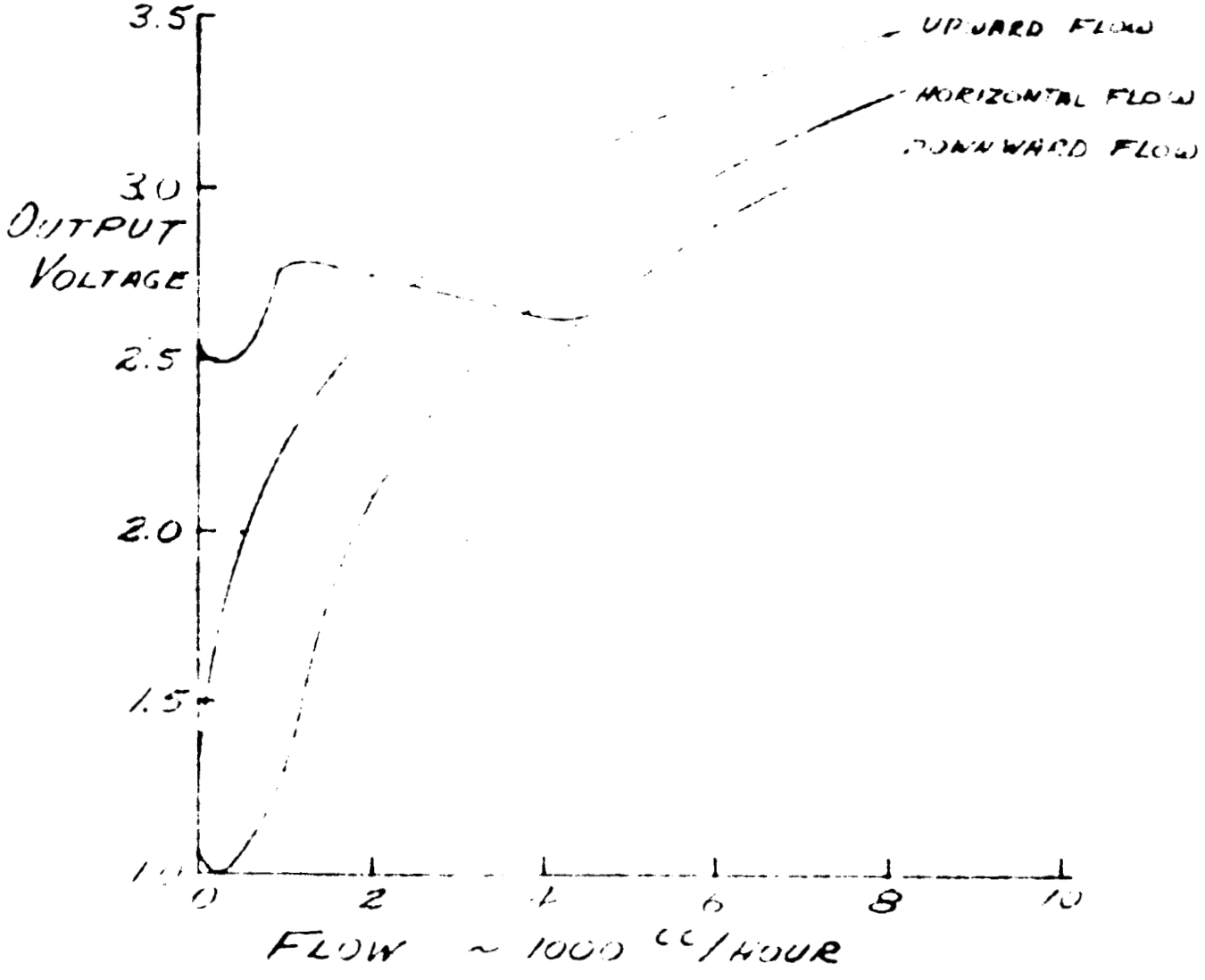

FIG 30

A resistor was installed between the two thermistors and the assembly was sealed with epoxy. The thermistors were connected in a bridge circuit and data were taken of output current as a function of flow rate. The data are presented in Figure 31. Although the performance of this first thermal differential transducer was somewhat erratic due to imperfect sealing of the electrical connections, the sensitivity at low flow rates was encouraging but not as high as expected from the analysis. This was decided to be due to the combined effects of free convection, the internal geometry of the meter, and the low temperature rise of the resistor.

A new transducer was constructed consisting of three glass thermistor probes closely spaced along the axis of a 1/2-inch outer diameter copper tube. The central thermistor was used as a heater and supplied with 113 mw. Testing indicated repeatable performance, good sensitivity at low flow rates and a positive leakage indication over a wide range of flow rates. Figure 32 shows the performance of this transducer.

After conducting further tests on different versions of the thermal differential transducer, it was decided to test a configuration in which the heater and thermistors were enclosed in stainless steel tubes mounted across the flow stream. This configuration was selected because it could serve as the basis of a practical, propellant compatible design. Figure 33 presents the performance of the transducer. The output signal provided suitable flow indication over the specified range of leakage rates from 25 cc/hour through 1800 cc/hour. The output signal rises at low flow rates as the temperature differential between the upstream and downstream measurement points increases. At flow rates above 800 cc/hour, the magnitude of the signal begins to decrease as the cooling effect of the flow

LOW RANGE
TRANSDUCER PERFORMANCE

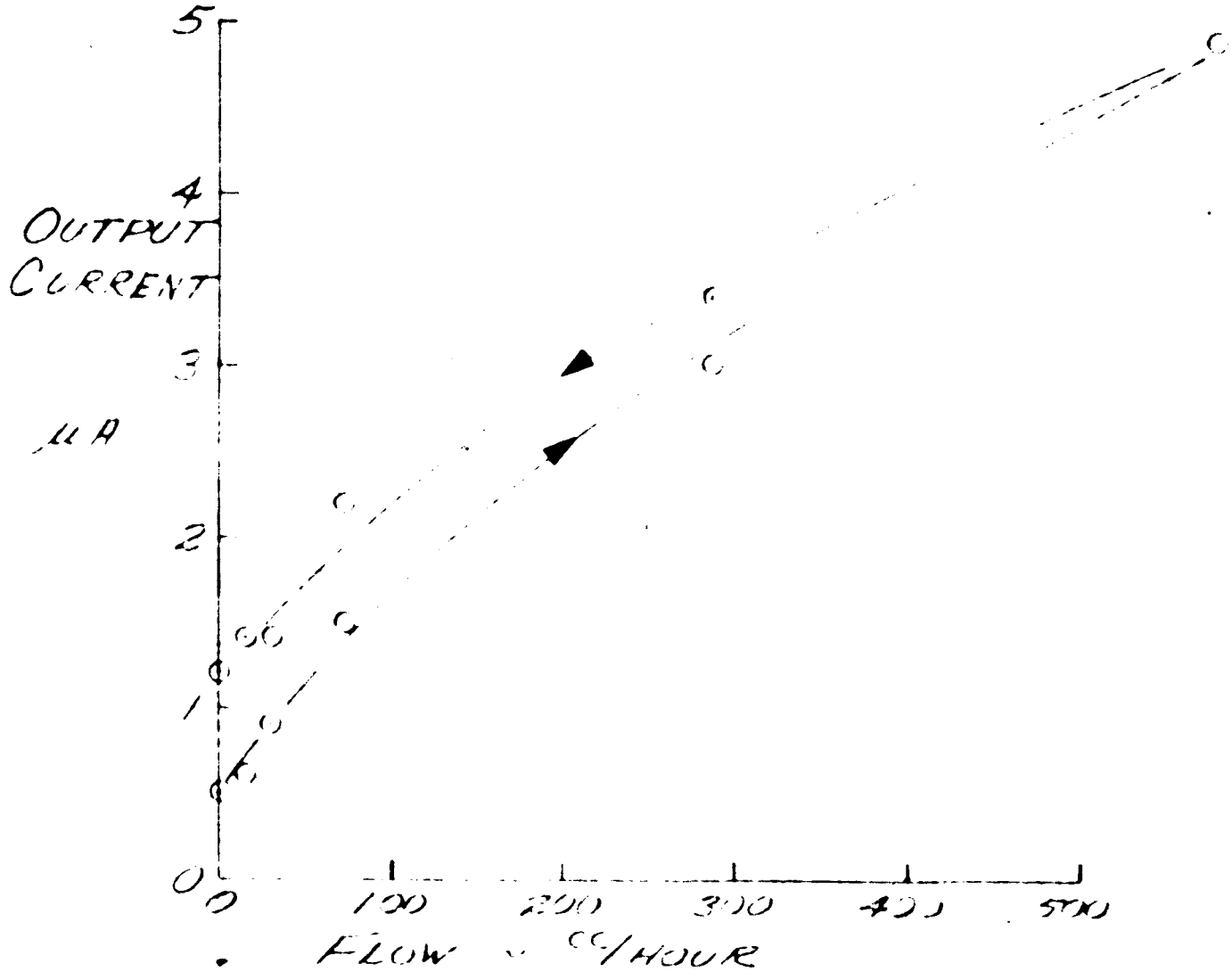

FIG. 31

LOW RANGE

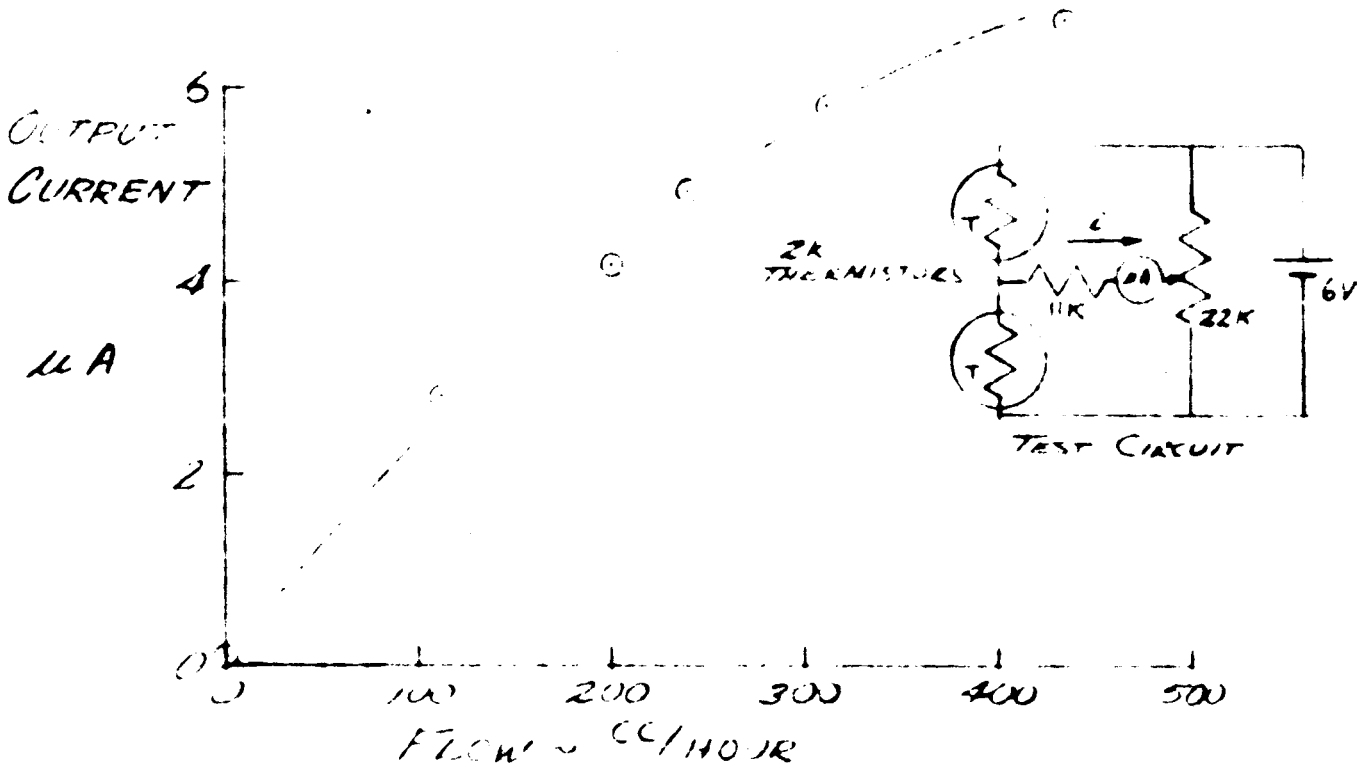

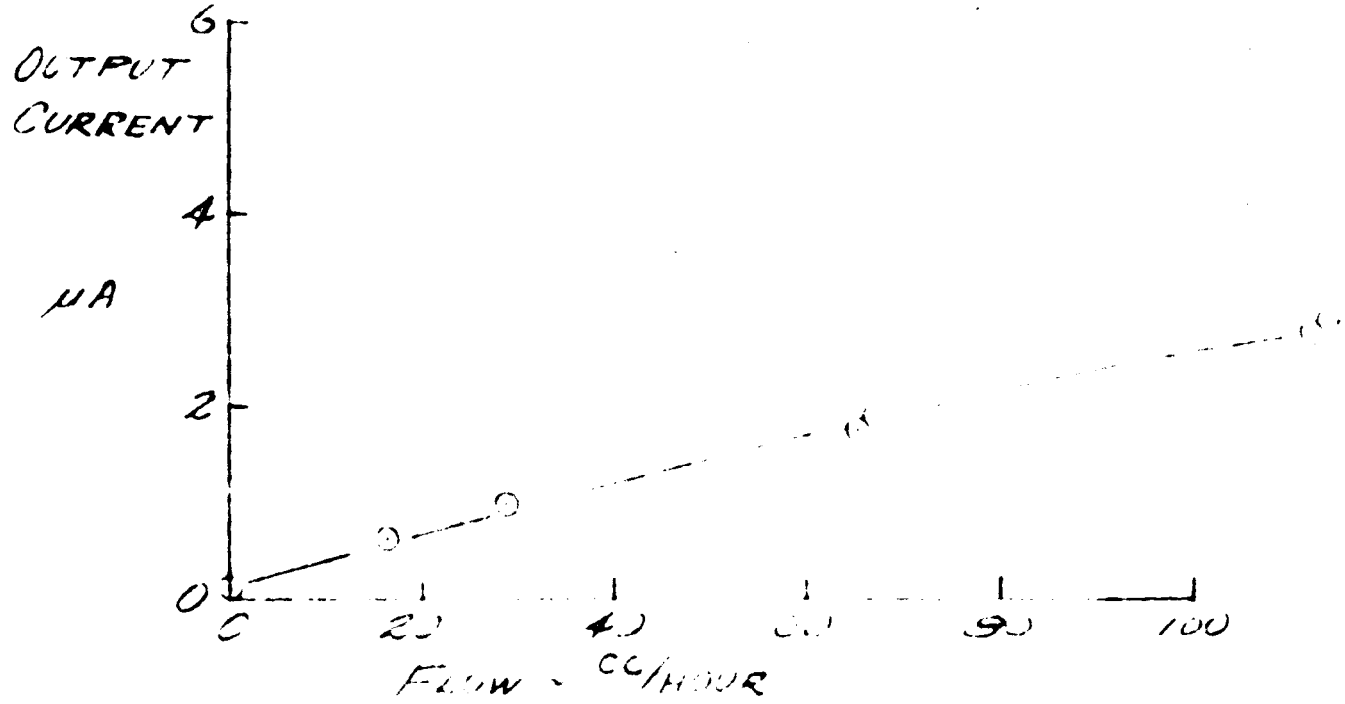

FIG. 32

CROSS TUBE
K RANGE TRANSDUCER

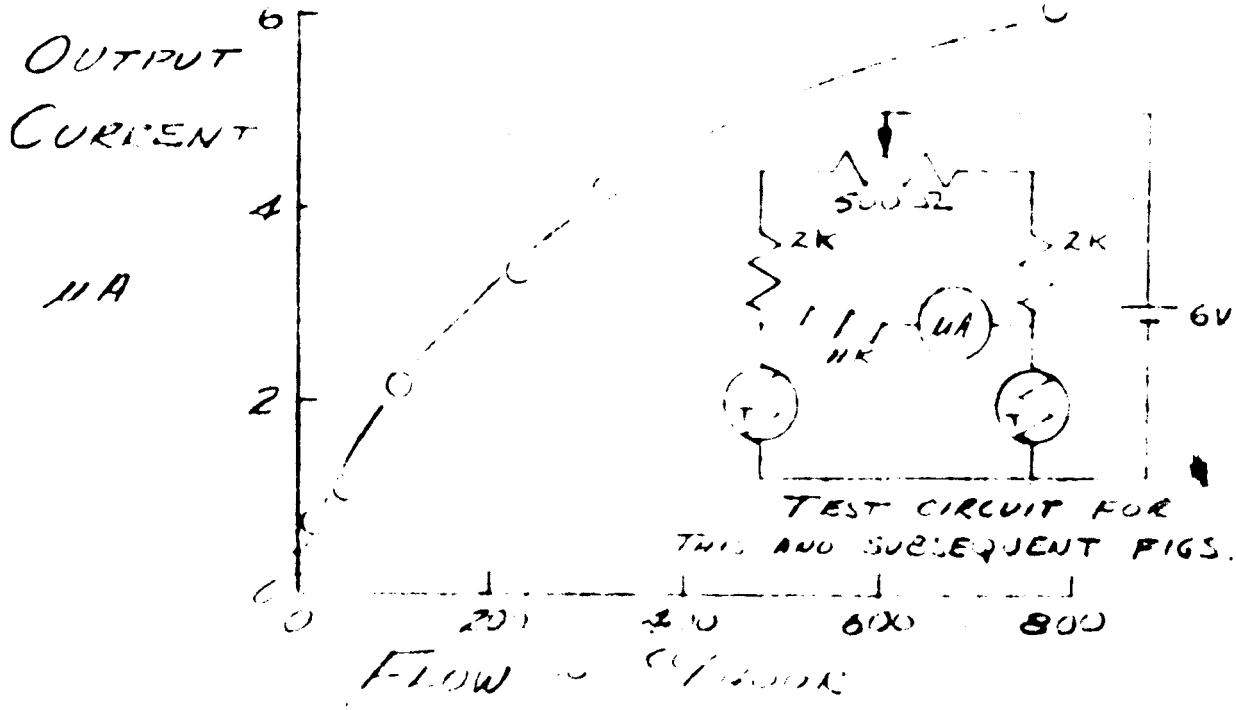

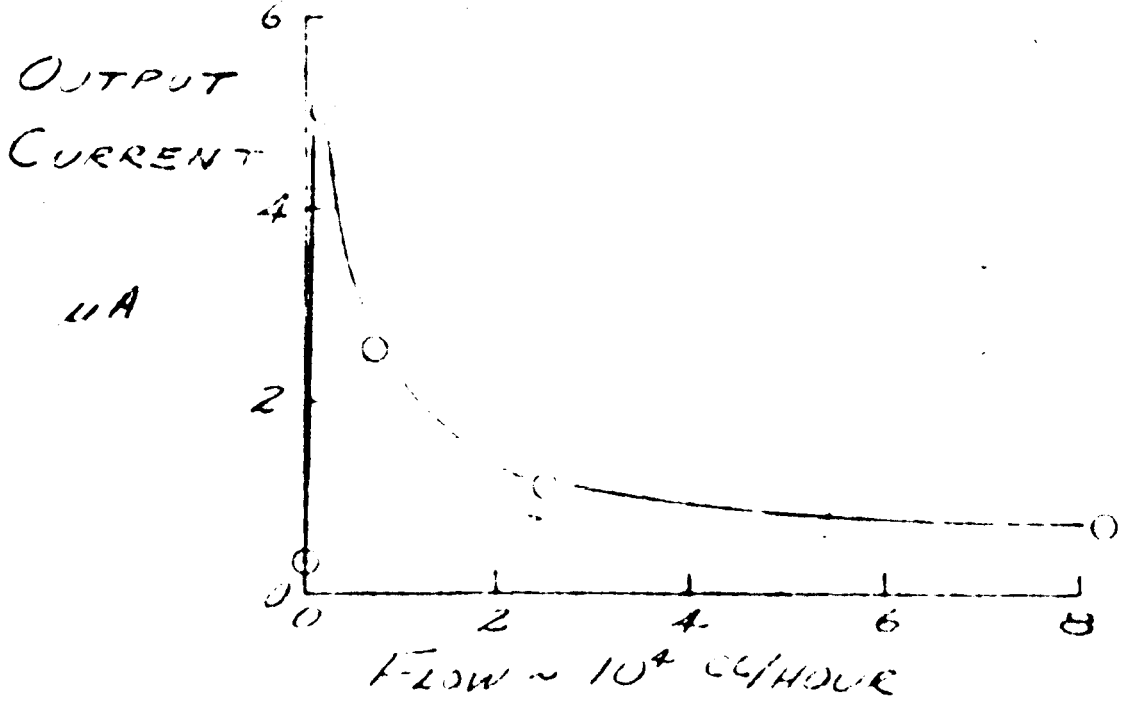

FIG 33

reduces the temperature of the heater. However, the leakage indication is more than adequate even at flow rates several times the required 1800 cc/hour. The individual temperatures of the upstream and downstream sensors were also measured. These data were used in conjunction with an analytical study in which moving heat source analysis was used to estimate the theoretical low flow threshold of the transducer in the absence of free convection.

Since the thermal differential transducer with elements enclosed in cross-stream tubes appeared to provide a practical approach to the low leakage rate detection problem, the experimental program was directed toward the establishment of a configuration for a high range transducer. This transducer would cover the range from 1000 cc/hour to 0.88 lbs/second, and would provide leakage detection and O/F ratio monitoring.

A transducer was made by winding heater and sensor windings around the periphery of a stainless steel tube. The nominal wall thickness of the tube was 0.026 inches. The nominal diameter was 3/4-inch. The wall thickness was reduced to approximately 0.005 to 0.007 inches over a 1 inch length. The heater and associated downstream sensor were wound in the center of this reduced wall thickness segment to limit axial heat conduction through the tube walls. The windings were impregnated with silicone oil to provide good thermal contact with the tube walls. A power of 1.4 watts was applied to the heater and data were taken of heater temperature rise above the fluid temperature as a function of flow rate. These data were gathered by monitoring the output of a bridge circuit that included the upstream and downstream sensor windings which were made with temperature sensitive (Balco) wire. The data for measurement of 55°F and 135°F water flow are presented in Figure 34.

TEMPERATURE RISE OF EXTERNAL HEATER

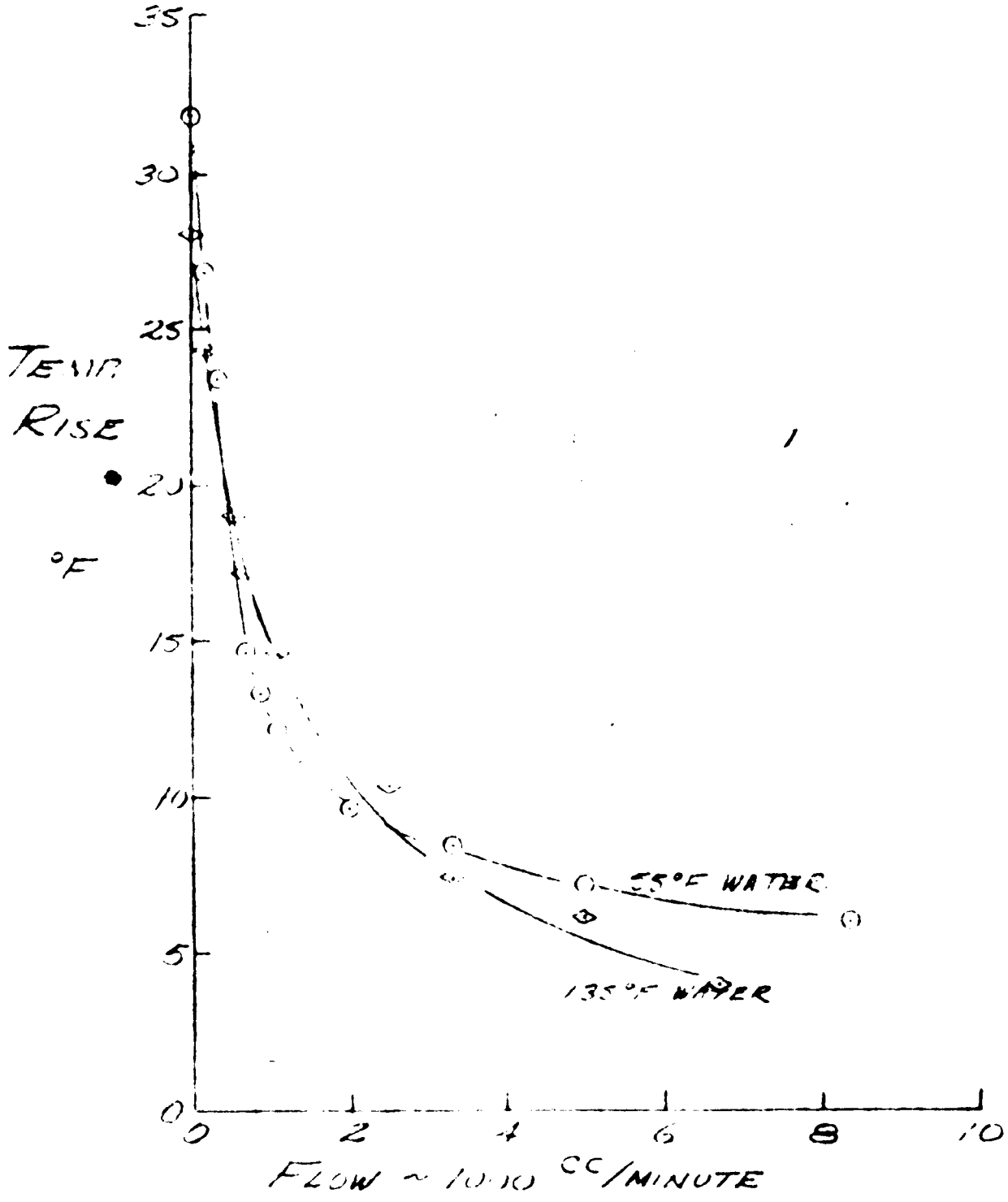

FIG 34

WALL HEAT TRANSFER COEFFICIENT

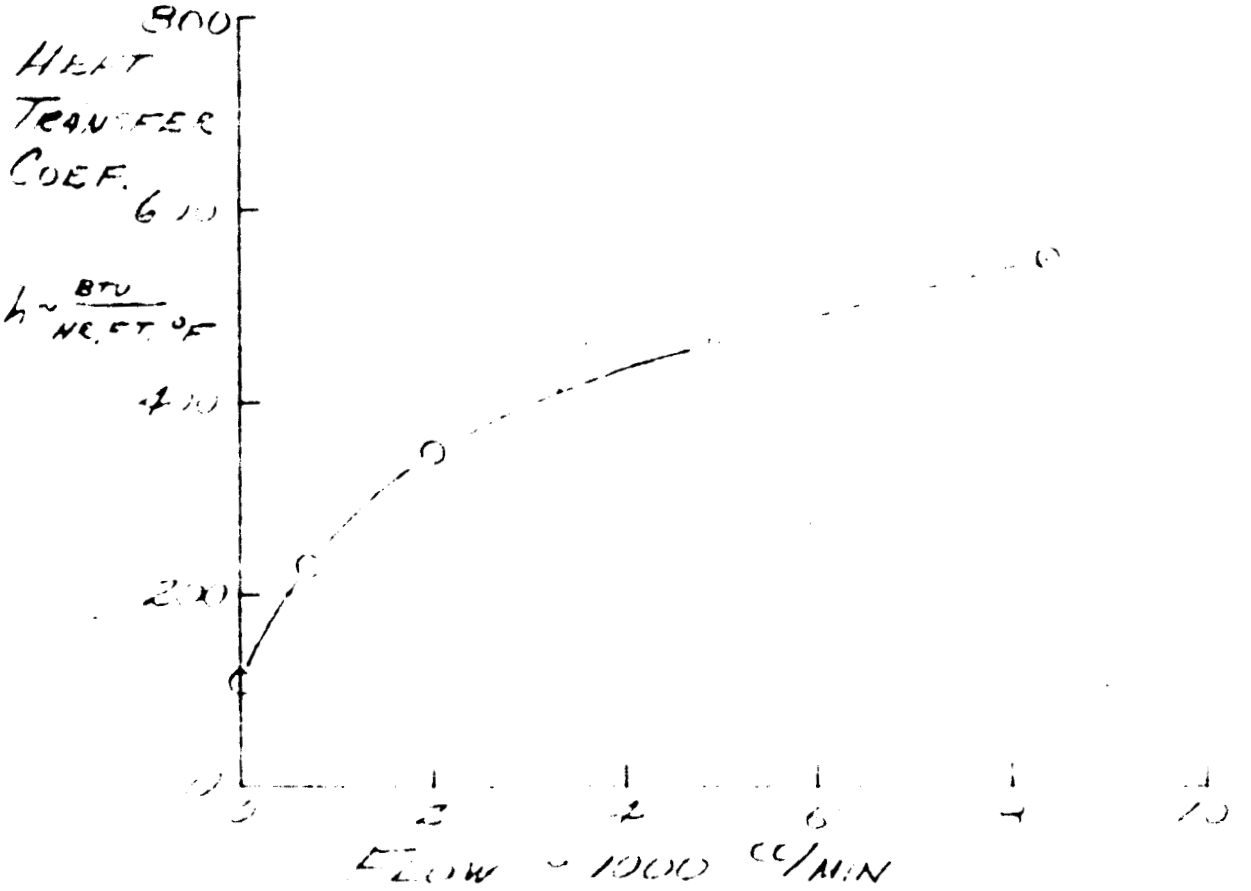

FIG 35

The heat transfer coefficient variation with flow rate was calculated from the temperature rise, heater power and estimated heater surface area. Figure 35 shows the variation of heat transfer coefficient with flow rate. These data are in good agreement with the values predicted analytically.

This high range transducer did provide good performance over the required range of flow rates and temperates. The low temperature coefficient of the Balco wire (0.45%/°C compared to 3.9%/°C for the thermistors) and the large heater power required to raise the temperature of the large heated area a sensible amount were felt to be liabilities in the PLDS application.

A transducer was constructed using thermistor temperature sensors and a resistance heater enclosed in stainless steel tubes mounted across a 1/2-inch copper tube. The surface temperature of the tube containing the heater was measured by bonding a thermistor-carrying tube to the surface of the heater tube. This technique effectively enclosed the thermistor in an isothermal surface which was at the same temperature as the surface of the heater. This approach was selected after experiencing difficulty with other methods of measuring heater temperature. The problem arises because the value of heat transfer coefficient between the tube wall and the fluid is so low that any measurement technique in which much of the heat passes through the temperature sensing thermistor makes the thermistor temperature insensitive to flow. This precludes placing the thermistor in the same tube with the heater.

Data were taken showing the performance of this transducer while measuring flow rates of 55°F and 135°F water. The data show adequate sensitivity for detecting leaks of 1000 cc/hour combined with the ability to measure full RCS system flow rates. These data are presented in Figure 36.

HIGH RANGE
CROSS TUBE SENSOR
IN
½" O.D. COPPER TUBE

.5 WATT HEATER

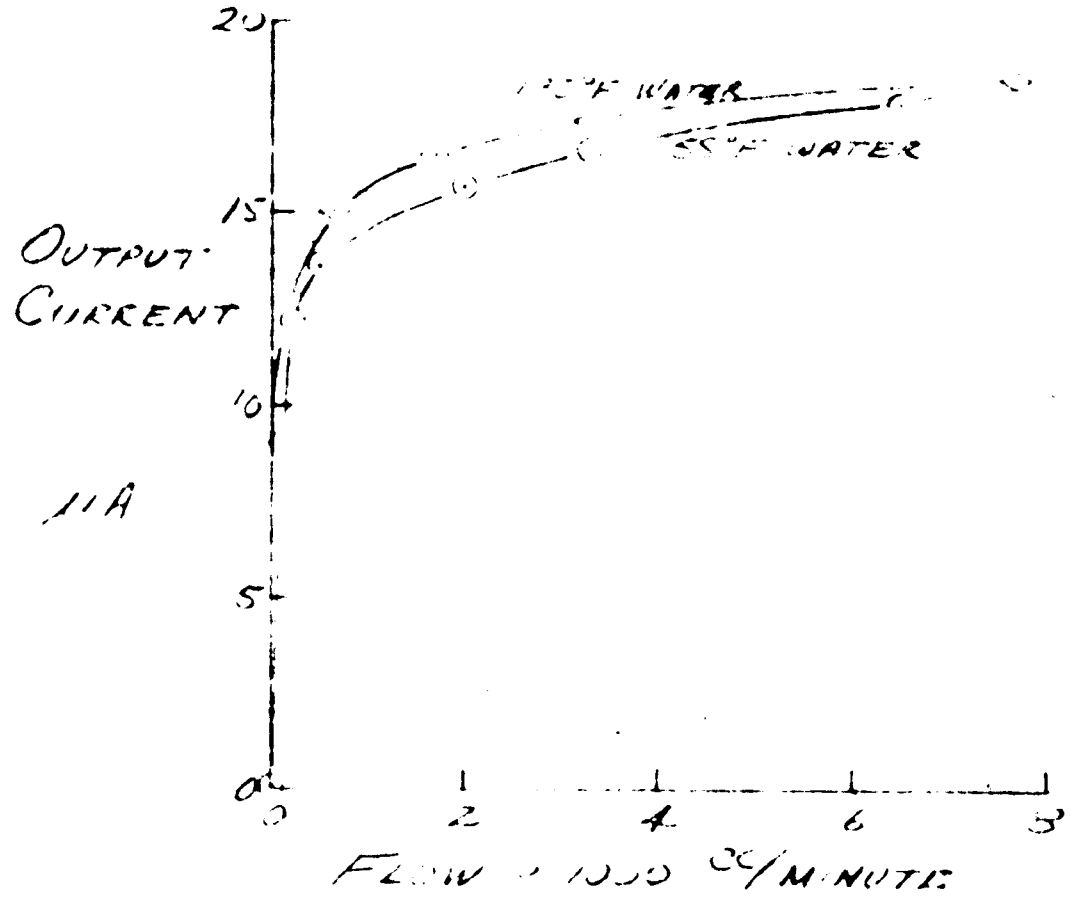

FIG. 36

The next step in the experimental program was to fabricate and test pre-prototype transducers made from the same materials as those contemplated for the end-item hardware. Such tests would ensure that the change to materials with different thermal properties (such as stainless steel instead of copper) would not degrade the performance of the low and high flow transducers.

The elements for low and high range leakage measurements were installed in a single 3/4-inch outer diameter stainless steel tube. The tube wall thickness was 0.026 inches. The thermistors and resistors were installed in cross-stream-mounted tubes of approximately 0.100 inch outer diameter and 0.010 inch wall thickness. These smaller tubes were mounted in place with epoxy. The heater and downstream sensor tubes for the high flow sensor were also joined together with epoxy.

The first test data taken with the low flow sensing system are presented in Figure 37.

The sensitivity at low flow rates was lower than desired so it was decided to investigate the influence of changing the heater power in the hope that the sensitivity might be increased. A series of tests was conducted in which the change in output current from the low flow sensing bridge was recorded as the flow rate was increased from 0 to 600 cc/hour. This was done for a number of different heater power levels. The resulting data are presented in Figure 38 and show that an increase in heater power level sometimes caused a decrease in flow sensitivity. The sensitivity versus power relation began to deviate from the expected straight line at about 100 milliwatts for 55° water temperature and at even lower power levels when the water was heated to 130°F.

LOW RANGE
PRE-PROTOTYPE
(NO BAFFLES)

.5 WATT HEATER

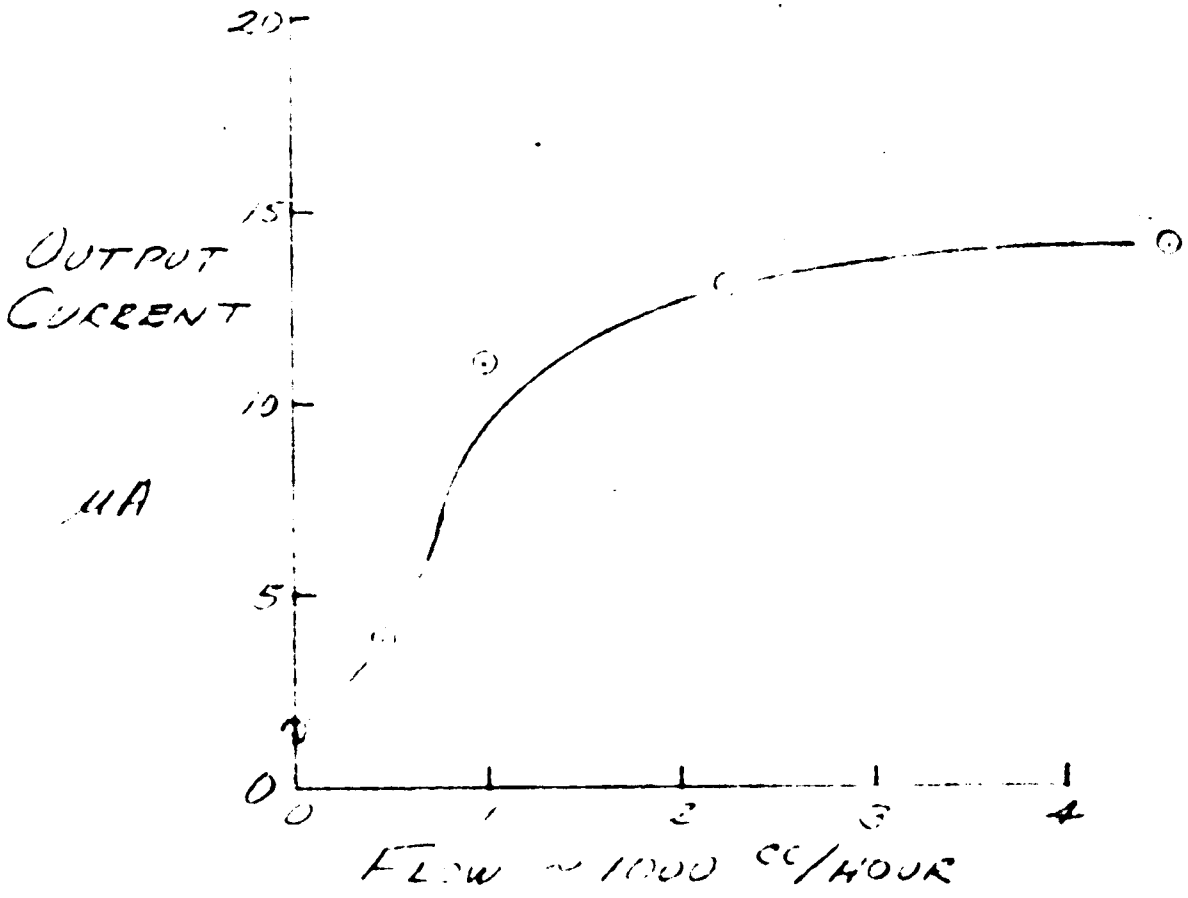

FIG 37

EFFECT OF HEATER POWER ON SENSITIVITY

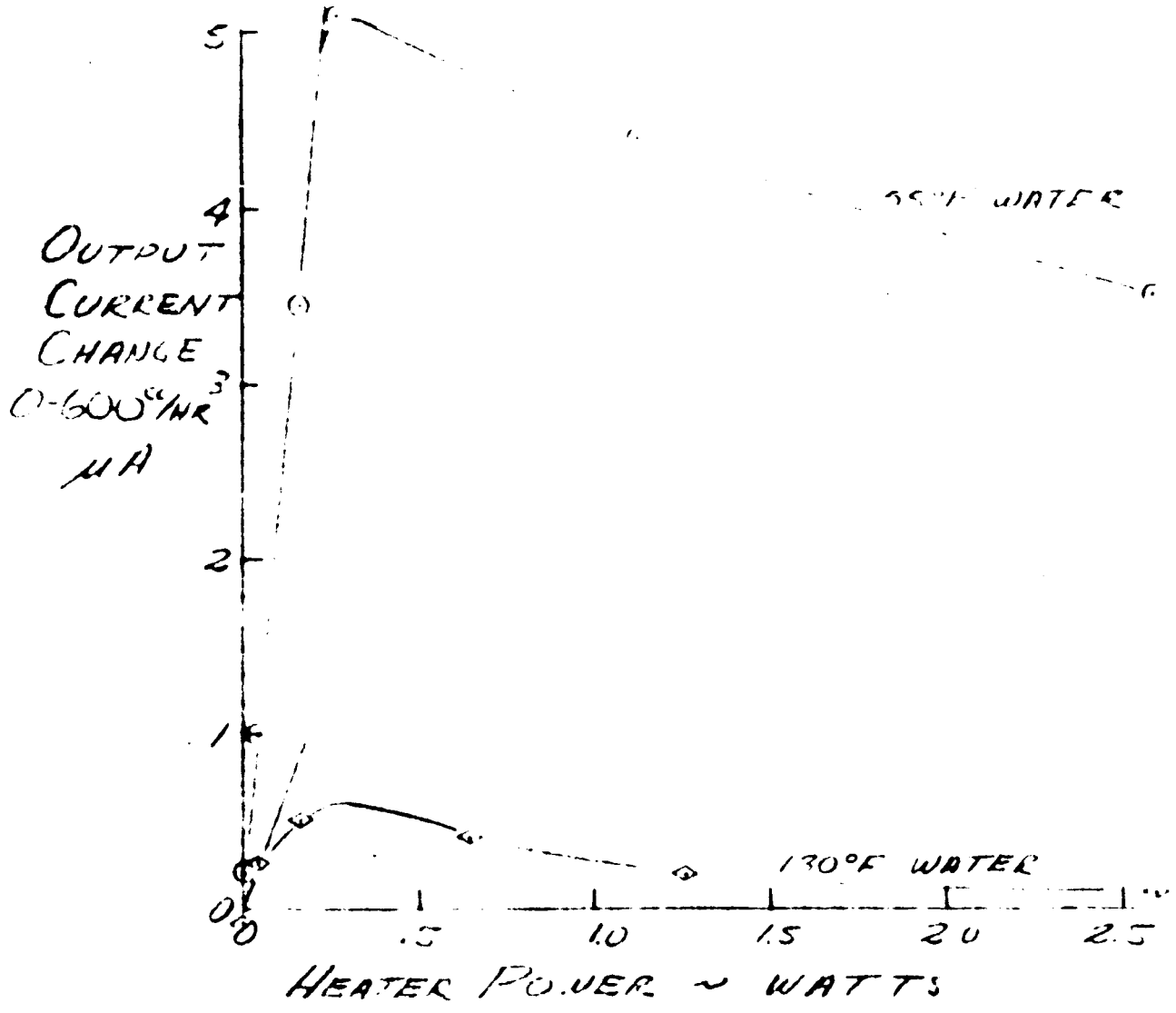

FIG 38

Analysis of the experimental data led to the conclusion that the anomalous behavior was due to the influence of free convection. The free convection velocities were calculated and found to be much higher than the flow velocities being measured. A small change in velocity due to flow was masked by the effects of the free convection. Raising the heater power tended to increase the free convection by increasing the temperature difference available to drive convection currents. Increasing the fluid temperature changed the fluid properties and also increased the free convection.

Although free convection would not affect the performance of the low range system in its intended gravity-free service environment, it was decided to limit the free convection so that the calibrations and system performance would more closely resemble the expected zero-G performance. Thin convection baffles were then fabricated and located on each side of the heater to prevent free circulation of the heated fluid in non-axial directions.

The low range system was then retested. The resulting data are presented in Figure 39 and show the expected marked increase in sensitivity at low flow rates. Some free convection effects were still present (as indicated by the decrease in sensitivity at high temperatures) but the sensitivity of the transducer in the range of temperatures expected was more than adequate.

The high range section of the pre-prototype transducer was then tested over the range of flow rates from 0 to 10,000 cc/minute. The resulting data are presented in Figure 40 and indicate satisfactory performance in both leakage and RCS flow ranges (Appendix C shows that the properties of the propellants are such that the propellant flow rate which corresponds to the same output signal as a given water

LOW RANGE
PRE-PROTOTYPE

(BAFFLES INSTALLED)

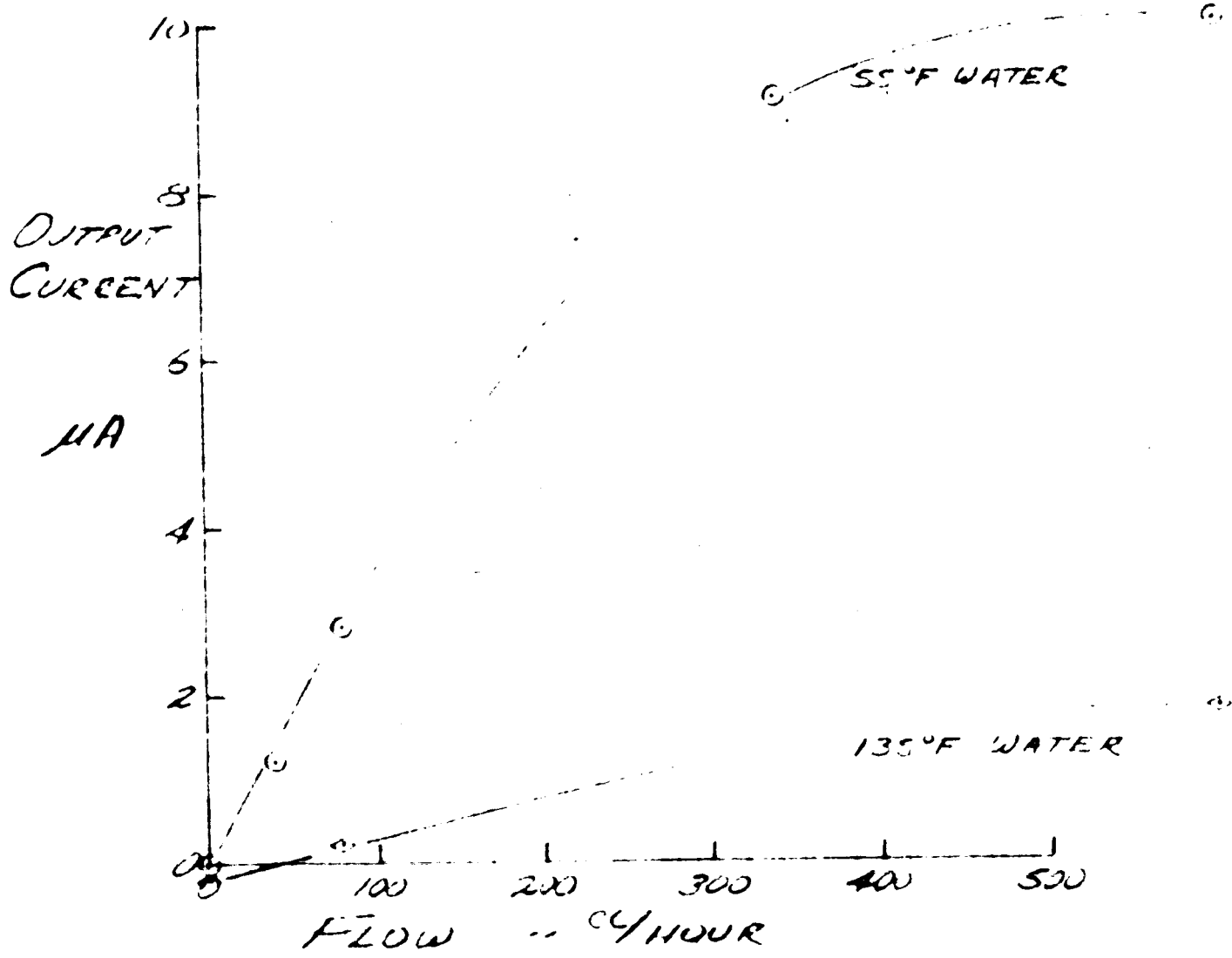

FIG. 39

HIGH RANGE
PRE-PROTOTYPE

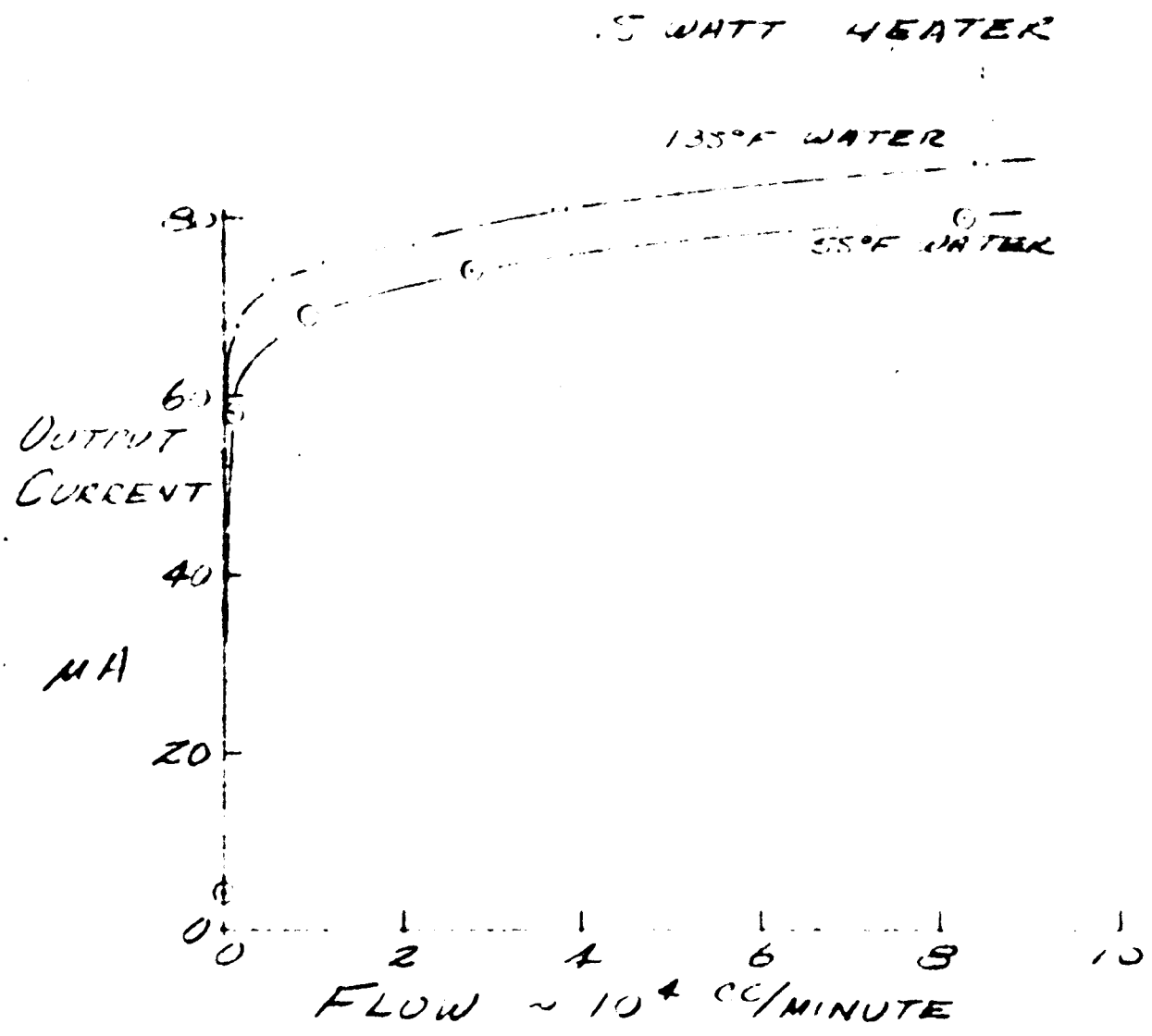

FIG. 40

flow rate is approximately twice as great). Figure 40 also shows that the effects of changing fluid temperature were moderate and within the range of easy compensation.

The performance of both the low and high range systems in the 3/4-inch stainless tube were considered satisfactory and it was therefore decided that deliverable prototype transducers would be fabricated and evaluated.

APPENDIX C

ANALYTICAL STUDIES

This Appendix contains some of the more important analytical studies performed during the program.

BASIC PERFORMANCE ANALYSIS

I Lowest Flow Range - 25 cc/Hr - 35 cc/Hr

A. Fuel

At 25 cc/Hr through a 3/4" ID pipe, the Reynolds number of the fuel is:

$$R_{e_F} = \frac{\rho V d}{\mu}$$

$$= \frac{4 \dot{W}}{\pi \mu d}$$

$$= \frac{4 \times 25 \times 0.898}{\pi \times 8.17 \times 10^{-3} \times 0.75 \times 2.54} \quad \frac{cm^3 \text{ gram Hr poise cm sec}}{\text{Hr } cm^3 \text{ poise cm } 3600 \text{ sec gram}}$$

$$= \underline{\underline{0.510}}$$

The nominal Prandtl number of the fuel is:

$$P_{r_F} \cong \underline{\underline{10}}$$

The Nusselt Number is:

$$Nu = \frac{hd}{k} = 3.65 + \frac{0.0665 \left(Re\ Pr \frac{d}{x}\right)}{1 + 0.04 \left(Re\ Pr \frac{d}{x}\right)^{2/3}}$$

For:

$$\frac{d}{x} \cong 10$$

We have:

$$Re\ Pr \left(\frac{d}{x}\right) \approx 510$$

and:

$$Nu = 3.65 + \frac{3.391}{1 + 2.56} = \underline{\underline{4.60}}$$

The heat transfer coefficient is then:

$$h_F = 4.60 \frac{k}{d}$$

$$= 4.60 \frac{0.1505}{0.75} \frac{\text{BTU}}{\text{Hr Ft°F}} \frac{12}{\text{Ft}}$$

$$= \underline{\underline{11.1}} \frac{\text{BTU}}{\text{Hr Ft}^2}$$

The characteristic length for heating the fluid to 63% of the wall to stream difference is:

$$\lambda = \frac{\dot{W} Cp}{\pi a h}$$

$$= \frac{Re \mu Cp}{4h}$$

Substituting for h:

$$\frac{\lambda}{d} = \frac{Re Pr}{4 Nu}$$

$$= 0.0543 Re Pr$$

For the present case:

$$\left(\frac{\lambda}{d}\right)_F = 0.0543 \times 0.510 \times 10$$

$$= 0.277$$

Or:

$$\lambda_F \cong \underline{\underline{0.21"}}$$

Thus, for a heater on the order of 75 mils in length, the meter will behave substantially as a Laub Meter and not as a Thomas Meter. The power

input will be(at 10°F differential)

$$q_F = hA\,(T_W - T_F)$$

$$\cong 11.1 \frac{BTU}{Hr\ Ft^2 {}^\circ F} \times \frac{\pi \times 0.75 \times 0.075 \times 10\ in^2 {}^\circ F}{144 in^2/Ft^2} \times \frac{1000\ mw}{3.413\ BTU/hr}$$

$$= \underline{\underline{29.2}}\ \text{milliwatts}$$

B. Oxidizer

At 35 cc/Hr through a 3/4" ID pipe, the Reynolds number of the oxidizer is:

$$Re_o = \frac{4 \times 35 \times 1.432}{\pi \times 0.410 \times 10^{-2} \times 0.75 \times 2.54 \times 3600}$$

$$= \underline{\underline{2.270}}$$

The nominal Prandtl number of the oxidizer is:

$$Pr_o \approx \underline{\underline{5}}$$

$$Re\ Pr \frac{d}{x} \cong 2.27 \times 5 \times 10$$

$$= \underline{\underline{113.5}}$$

$$Nu_o = 3.65 + \frac{0.0665 \times 113.5}{1 + (0.04 \times 113.5^{2/3})}$$

$$= 3.65 + \frac{7.548}{1.936}$$

$$= \underline{\underline{7.55}}$$

$$h_o = \frac{7.55 \times 0.0755 \times 12}{0.75}$$

$$= \underline{\underline{9.12}} \frac{BTU}{Ft^2\ Hr}$$

$$\frac{\lambda_o}{d} = \frac{2.27 \times 5}{7.55 \times 4}$$

$$= 0.375$$

$$\lambda_o = \underline{\underline{0.28"}}$$

$$q_o = \frac{9.12 \times \pi \times 0.75 \times 0.075 \times 10 \times 10^3}{144 \times 3.413}$$

$$= \underline{\underline{24.0}} \text{ milliwatts}$$

II Malfunction Condition

A. Fuel - 1350 cc/Hr

$$Re_F = \underline{\underline{27.540}}$$

$$Re\ Pr\ \frac{d}{x} = 2754$$

$$Nu_F = 3.65 + \frac{183.14}{1 + 7.848}$$

$$= \underline{\underline{24.35}}$$

$$\lambda_F = \frac{0.75 \times 27.54 \times 10}{24.35}$$

$$= \underline{\underline{8.48"}}$$

$$h_F = \underline{\underline{58.76}}\ \frac{BTU}{Hr\ Ft^2}$$

$$q_F = \underline{\underline{154.6}} \text{ milliwatts}$$

B. Oxidizer - 1700 cc/Hr

$$Re_o = \underline{\underline{110.3}}$$

$$Re\ Pr \frac{d}{x} = 5513$$

$$Nu_o = 3.65 + \frac{366.6}{1 + 12.48}$$

$$= \underline{\underline{30.85}}$$

$$\lambda_o = \frac{0.75 \times 110.3 \times 5}{30.85}$$

$$= \underline{\underline{13.4"}}$$

$$h_o = \underline{\underline{37.3}}\ \frac{BTU}{Hr\ Ft^2}$$

$$q_o = \underline{\underline{98.0}}\ \text{milliwatts}$$

III Full Flow

A. Fuel - 0.44 #/sec

$$Re_F = \frac{0.44 \times 4\ \#/sec \times 12"/Ft}{\pi \times 0.75" \times 8.17 \times 10^{-1}\ Cp \times 6.72 \times 10^{-4}\ \frac{\#}{Sec\ Ft}}$$

$$= \underline{\underline{16,326}}$$

The flow is turbulent. From Diessler, we see that:

$$Nu_{Av} = 2.36\ Nu_\infty$$

For:

$$Pr = 10 \quad \text{and} \quad Re = 16,000 \quad \text{and} \quad \frac{d}{x} = 10$$

the Dittus-Boelter Equation gives:

$$Nu_o = \frac{hd}{k} = 0.0243\, Re^{0.8}\, Pr^{0.4}$$

$$= 143$$

$$Nu_{Av} = \underline{\underline{338}}$$

$$h = \underline{\underline{812.8}}\ \frac{BTU}{Ft^2 Hr}$$

$$q_F = \underline{\underline{2.14}}\ \text{watts}$$

B. Oxidizer - 0.88 #/sec

$$Re_o = \frac{4 \times 0.88 \times 12}{\pi \times 0.75 \times 6.72 \times 10^{-4} \times 0.41}$$

$$= \underline{\underline{65,066}}$$

$$Nu_{Av} = 2.20\, N_{u_o}$$

$$Nu_o = 0.0243\, Re^{0.8}\, Pr^{0.4}$$

$$= 327.6$$

$$Nu_{Av} = \underline{\underline{720.7}}$$

$$h_o = \underline{\underline{871}}\ \frac{BTU}{Hr\ Ft^2}$$

$$q_o = \underline{\underline{2.29}}\ \text{watts}$$

IV Heat Leaks

A. Radial Heat Leak

$$Q \cong \frac{k}{x} \; A \, \Delta T$$

If air is the insulator and $x \cong 0.1$ inches

$$Q = \frac{0.015 \times \pi \times 0.75 \times 0.75}{0.0083 \text{ Ft } 144} \; \frac{\text{BTU}}{\text{Hr Ft °F in}^2} \; \frac{\text{Ft in}^2 \; 10\text{°F } 1000\text{mw Hr}}{3.913 \text{ BTU}}$$

$$Q = \underline{\underline{6.47}} \text{ mw}$$

B. Axial Heat Leak Through Fuel

$$Q = (k_w A_w + K_f A_f) \; \frac{\Delta T}{l}$$

The problem is to develop a significant value of l. The exact approach would involve describing the entire thermal picture including axial and radial conduction. As an approximation, we will assume that $l \cong d$.

$$Q = (10 \, \pi \, dt + 0.15 \, \frac{\pi}{4} d^2) \; \frac{\Delta T}{l}$$

$$Q = 3.14 \times 10^{\circ} \left(10 \times \frac{10^{-3}}{12} + 0.15 \times \frac{0.75''}{12 \frac{\text{in}}{\text{ft}} \times 4}\right) \frac{\text{BTU}}{\text{Hr Ft}}$$

$$\times \frac{1000}{3.413} \; \frac{\text{mw/hr}}{\text{BTU}}$$

$$Q = 9.2 \times 10^3 \, (0.883 + 2.34) \times 10^{-3}$$

$$Q = \underline{\underline{29.2}} \text{ mw}$$

This is equal to the low threshold signal.

C. Axial Heat Leak Through Oxidizer

$$Q = 3.14 \times 10 \left(10 \times \frac{10^{-3}}{12} + \frac{0.0755 \times 0.75}{12 \times 4}\right) \frac{1000}{3.413}$$

$$Q = \underline{\underline{18.5}} \text{ mw}$$

This is comparable to the threshold signal.

EFFECT OF FLUID PROPERTIES IN TURBULENT FLOW

Steady Flow Nusselt Number

The heat transfer coefficient will depend primarily on the Reynolds number and the Prandtl number of the flow. The L/D of the heated section will affect the value of h, but the effect of L/D does not change greatly with Re or Pr in turbulent flow. In laminar flow the heat transfer coefficient is a direct function of Re Pr $(\frac{d}{l})$.

The first step in evaluating the effect of varying fluid properties is to examine the equations for h and the variation of Re and Pr over the range of ambient conditions expected. For steady turbulent flow Eckert and Drake[1] give:

$$Nu \cong 0.0243\, Re^{0.8}\, Pr^{0.4} \qquad (1)$$

This does not include the effects of L/D, but does indicate the effect of Re and Pr variation.

Hausen gives an expression for average Nusselt number which does include the effects of L/D, but does not reduce to the Dittus-Boelter Equation (1) for large L/D.

$$Nu = 0.116\, (Re^{2/3} - 125)\, (Pr^{1/3}) \left[1 + \left(\frac{d}{x}\right)^{2/3}\right] \left(\frac{\mu_B}{\mu_w}\right)^{0.14} \qquad (2)$$

This expression also accounts for the viscosity at the wall being different from the bulk values. Although Equations (1) and (2) are not quite the same, the effect

- - - - - - - - - - - - - - - -

[1] Eckert, E. R. G., and R. M. Drake, Jr., Heat and Mass Transfer, McGraw-Hill Series in Mechanical Engineering, 1959.

of varying fluid properties is virtually identical in both equations.

Fluid Properties

The significant fluid properties for the present application can be grouped from Equation (1) as:

$$h \alpha k^{0.6} \left(\frac{Cp}{\mu}\right)^{0.4} \qquad (3)$$

The required temperature range for the propellants is from their melting points which are about 20°F to 140°F.

The properties of N_2O_4 and 50% UDMH-N_2H_4 are tabulated below.

T	N_2O_4				50% UDMH-N_2H_4			
	k	Cp	μ	$\frac{h}{h_{77}}$	k	Cp	μ	$\frac{h}{h_{77}}$
°F	BTU/Hr Ft°F	BTU/# °F	Cp	-	BTU/in Sec°F	BTU/# °F	Cp	-
77	0.0755	0.368(a)	0.410	1.000	0.346×10^{-5}	0.694	0.86(a)	1.000
40	0.0809	0.357	0.499	0.951	0.350	0.685	1.16	0.887
100	0.0715	0.376	0.342	1.050	0.344	0.704	0.76	1.053
140	0.0620	0.393	0.260	1.095	0.3395	0.715	0.59	1.164

(a) Values were obtained from curves - other values not noted with superscript (a) at 77° were taken from tables.

FLUID PROPERTY VARIATION
TABLE I

We see from Table I that the effect on heat transfer coefficient of fluid property

variation in the turbulent regime will be on the order of 7.5% for N_2O_4 and 16% for 50% UDMH-N_2H_4. The effect is described by a smooth curve, so that temperature compensation may be possible. It should be noted that the effective variation in flow rate will be greater than the variation of h, since the flow rate comes into the Nusselt Number expression to the 0.8 power. The overall effect on computed flow rate will be about 9.5% for N_2O_4 and 20% for 50% UDMH-N_2H_4 based on the average properties.

The effect of varying fluid properties on laminar flow are much less than for turbulent flow, since viscosity effects drop out.

PROPELLANT TO WATER CONVERSION FACTORS FOR TURBULENT FLOW

This analysis calculates the water flow rates which will give the same signal as the expected RCS flow rates. The proportionality between heat transfer and the flow and fluid properties is given by:

$$h \sim \frac{k}{d} \; Re^{0.8} \, Pr^{0.31}$$

This may be written:

$$h \sim \frac{k}{d} \; \left(\frac{\rho V d}{\mu}\right)^{0.8} \left(\frac{\mu Cp}{k}\right)$$

Or:

$$h \sim \frac{k^{0.69} Cp^{0.31} (\rho V)^{0.8}}{d^{0.2} \mu^{0.49}}$$

The flowmeter signal will be identical for propellant and water flows provided that the heat transfer coefficients are the same. If h/hw = 1, we may write:

$$\frac{\rho V}{(\rho V)_w} = \left(\frac{\mu}{\mu_w}\right)^{0.61} \left(\frac{k_w}{k}\right) \left(\frac{C_{pw}}{C_p}\right)^{0.39}$$

For the oxidizer at 77°F:

$$\frac{\mu}{\mu_w} = 0.41$$

$$\frac{k_w}{k} = 4.6$$

$$\frac{C_{pw}}{C_p} = 2.72$$

Combination of these ratios with Equation (2) shows that 0.88#/sec of N_2O_4 may be simulated by 0.27#/sec of water flow.

Converting the equivalent water flow to cc/minute:

$$0.27\#/\text{sec} \times \frac{16.4\ \text{cc/in}^3}{62.4\#/\text{ft}^3} \times 1728\ \text{in}^3/\text{ft}^3 \times 60\ \frac{\text{sec}}{\text{min}} = 7380\ \text{cc/min}$$

For the fuel at 77°:

$$\frac{\mu}{\mu_w} = 0.86$$

$$\frac{k_w}{k} = 2.333$$

$$\frac{C_{pw}}{C_p} = 1.44$$

Proceeding as before, we find that 0.44#/sec of N_2H_4 may be simulated by 0.207#/sec of water flow (5630 cc/minute).

FREE CONVECTION VELOCITY

This analysis provides an estimate of the free convection velocities in the PLDS sensors.

Eckert and Drake (Ref. 1) gives the maximum velocity in the boundary layer around a heated vertical plate as:

$$U_{max} = 0.766\,\mu\,(0.952 + Pr)^{-1/2}\,\frac{g\beta\theta}{\mu^2}^{1/2}\,X^{1/2}$$

Where:

- μ is the kinematic viscosity
- Pr is the Prandtl number
- g is the acceleration due to gravity
- β is the expansion coefficient
- θ is the wall temperature
- X is the heated length for free convection

This may be written:

$$U_{max} = 0.766\,(0.952 + Pr)^{-1/2}\,(g\beta)^{1/2}\,\theta^{1/2}\,X^{1/2}$$

For water at 68°F:

$$Pr = 7.02$$

$$\beta = 10^{-4}\,{}^{\circ}R^{-1}$$

and:

$$U_{max} = 0.766\,(7.972)^{1/2}\,(32.2 \times 10^{-4})^{1/2}\,(\theta X)^{1/2}$$

Or:

$$U_{max} = 0.0154\,(\theta X)^{1/2}$$

For water at 140°F:

$$Pr = 3.02$$

$$U_{max} = 0.766\,(3.972)^{-1/2}\,(32.2 \times 10^{-4})^{1/2}\,(\theta X)^{1/2}$$

Or:

$$U_{max} = 0.0219\,(\theta X)^{1/2}$$

For a heated length of 0.6 inches and a temperature rise of 10°F, the free convection velocities are:

$$U_{max} = 0.011 \text{ ft/sec at } 68°F$$

$$U_{max} = 0.0155 \text{ ft/sec at } 140°F$$

The equivalent water flow rates in a 0.6 inch diameter tube are given by:

$$Q = U_{max}\,\frac{\pi d^2}{4}$$

At 68°F:

$$Q = 0.011 \times 3600 \times \frac{\pi \times 0.05^2}{4} \times 1728 \times 16.4$$

Or:

$$Q = 2220 \text{ cc/hour}$$

Similarly, at 140°F:

$$Q = 3100 \text{ cc/hour}$$

The introduction of baffles will reduce these equivalent flow rates by the square root of the ratio of the unobstructed distance before and after baffling. A 100 to 1 reduction in the factor (θX) will reduce the free convection flow rate equivalents to 222 and 310 cc/hour.

Ref. 1: Eckert, E. R.G. and Drake, R.M., "Heat and Mass Transfer." McGraw-Hill, 1959.

SUBMERGED ELEMENT ANALYSIS

A. Single Bead Thermistor Cooling Data

The use of glass beaded thermistors as temperature sensors for the leak meter is being considered. In order to obtain some data on the characteristics of these devices, a test was conducted to determine the temperature of the thermistor immersed in a stream of water as a function of flow. The data are tabulated below in Table I. The details of the test are described elsewhere by Spacelabs personnel. The only significant detail for analysis of the data is that the tube has a nominal inside diameter of 0.500 inches and the thermistor bead has a nominal diameter of 0.060 inches.

Flow Q cc/Hr.	Power P Milliwatts	Temperature ΔT °C	Apparent Heat Transfer Coefficient h_o BTU/Hr Ft^2°F
0	97.0	30	72.4
64	96.0	28	76.7
1,105	98.5	27	81.7
2,800	100.0	21	106.0
7,000	99.7	14	162.0
13,300	99.5	13	172.0

TABLE I

THERMISTOR BEAD DATA

B. Background Analysis

The thermal circuit here consists of two resistances in series. There is a temperature drop between the core of the bead and the surface. There is another temperature drop between the surface and the fluid. If we call h_k the "conduction coefficient" and h_s the surface coefficient, then:

$$h_o = \frac{1}{\frac{1}{h_k} + \frac{1}{h_s}} \tag{1}$$

The "conduction coefficient" is related to the structure of the bead. If the glass coating goes from radius "a" to radius "b" with a thermal conductivity "k_g", then the heat flux will be:

$$q = \frac{4\pi ab}{a-b} \; k_g \; (T_c - T_s) \tag{2}$$

So that the conduction coefficient will be:

$$h_k = \frac{q}{4\pi b^2 \Delta T} = \frac{a}{b-a} \; \frac{k_g}{b} \tag{3}$$

The external heat transfer coefficient depends on the properties of the flow. Fuchs gives a preferred form for a sphere in air of:

$$\frac{2h_s b}{k} = Nu_s = 2\,(1 + 0.276\,Re^{1/2}\,Pr^{1/3}) \tag{4}$$

McAdams shows a preferred form for fluids of:

$$Nu_s = Pr^{0.3}\,(0.97 + 0.68\,Re^{0.5}) \tag{5}$$

C. Interpretation of the Data

By plotting the experimental ΔT versus $\frac{1}{Q}$, we can obtain an estimate of the bead temperature limit as $Q \longrightarrow \infty$. This is done in Figure 1. It is seen in Figure 41 that as the flow increases, the temperature differential between the bead and the stream approaches 10.4°C. This corresponds to a value of h_o = 215 BTU/Hr Ft^2°F. Examination of the previous equations shows that as $Re \longrightarrow \infty$, $h_s \longrightarrow \infty$, so that $h_o \longrightarrow h_k$. Thus we must estimate that:

$$h_k = 215 \frac{BTU}{Hr\ Ft^2 °F} \qquad (6)$$

This corresponds to a value of "a" of about 0.019 inches. Having a value of h_k, we can now find h_s and plot it against Reynolds Number. This is done in Figure 42, based on the values tabulated in Table II.

Q	Re	h_o	h_s	Nu
0	0.0	72.4	109	1.55
64	0.41	76.7	119	1.70
1,105	7.15	81.7	132	1.89
2,800	18.1	106.0	209	2.99
7,000	45.2	162.0	657	9.36
13,300	86.0	172.0	861	12.3

TABLE II

The data in Figure 42 shows a moderate agreement with the theoretical values at both ends of the test range. This is comparable to the degree of correlation normally expected in this kind of data.

THERMISTOR EXPERIMENTAL DATA

TEMPERATURE RISE VERSUS HEAT FLUX

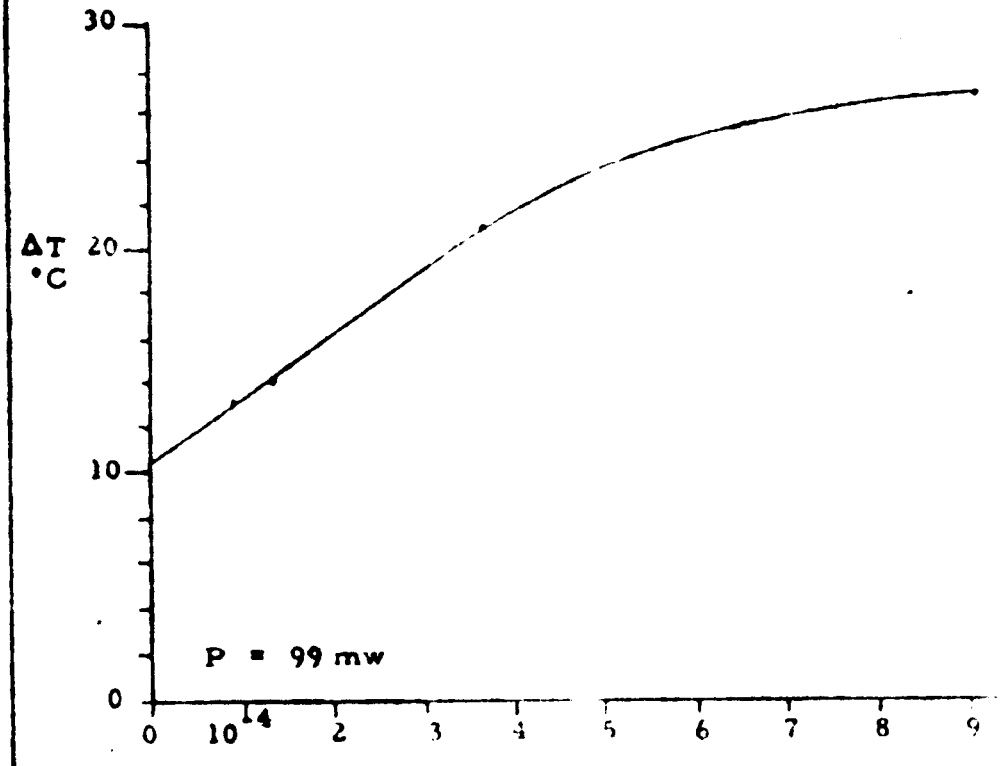

FIGURE 41

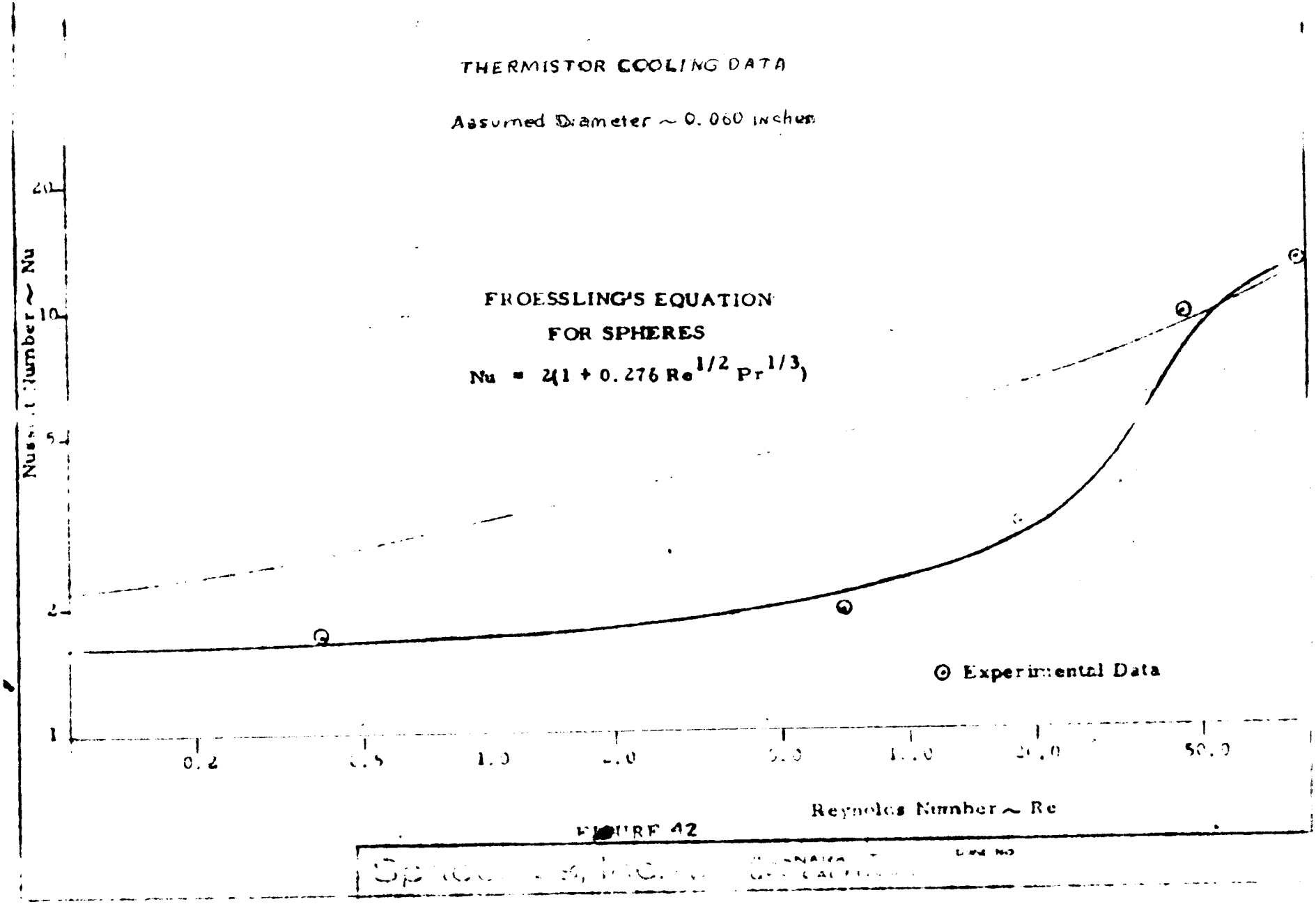
THERMISTOR COOLING DATA
Assumed Diameter ~ 0.060 inches
FROESSLING'S EQUATION
FOR SPHERES
Nu = 2(1 + 0.276 Re^1/2 Pr^1/3)
Nusselt Number ~ Nu
20
10
5
2
1
0.2
0.5
1.0
2.0
5.0
10.0
20.0
50.0
⊙ Experimental Data
Reynolds Number ~ Re

FIGURE 42

D. Significance of the Results

The importance of the test results is almost immediately evident from the temperature differential versus flow data. At low flows the bead sees a measurable change in temperature at the level of flow rates of interest and the low leakage rates. The bead "saturates" at flow much less than the 10^6cc/Hr which corresponds to the high flow signal. This saturation is due to the thermal resistance between the core of the bead and its surface. Internally generated heat may be useful for low flows, but is ruled out for high flow applications in the form tested here.

E. Three-Probe Meter

An experimental leak detector was designed and tested which used a central heater and two thermistors as shown in Figure 43. Each of the elements was encased in a steel hypodermic tube as indicated. Thermal contact between the elements and the tube wall was obtained by use of a silicone grease.

An analysis was conducted to establish the approximate characteristics of the meter. The first question was to find the approximate temperature which would be achieved using the meter in a stagnant fluid. The second question was to estimate the velocity effect on the meter.

F. Moving Source of Heat on a Line

An approach to estimating both the static and dynamic behavior of the meter was to assume that it acted like a source of heat moving through the fluid. This permits us to use existing solutions to that problem. Jakob shows that when a source of heat moves along a thermal conductor which has heat loss to the

EXPERIMENTAL LEAK DETECTOR

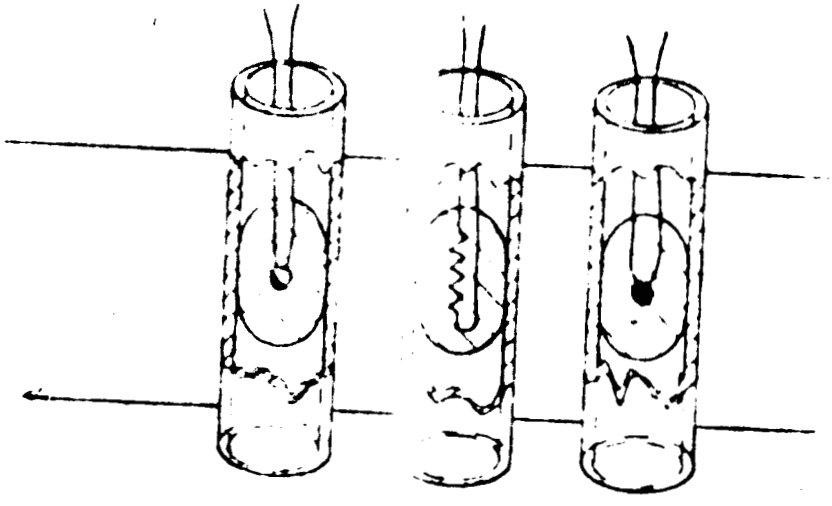

FIGURE 43

surroundings, the temperature distribution around the source is given by:

$$T = T_{max}\, e^{-(a+b)x} \quad \text{for } x < o$$

$$T = T_{max}\, e^{+(a-b)x} \quad \text{for } x < 0$$

Where:

$$a = \sqrt{m^2 + b^2}$$

$$b = \frac{v}{2\alpha}$$

$$\alpha = \frac{k}{\rho C_p}$$

$$m^2 = \frac{hC}{kA}$$

h - heat loss coefficient

C - circumference at loss surface

A - cross-section for heat flow

x - distance upstream of the source

The maximum temperature is related to the total heat flux by:

$$T_{max} = \frac{q}{2ka}$$

G. Zero Velocity

At v = o, the maximum temperature becomes:

$$T_{max} = \frac{q}{2km}$$

The temperature variation with position becomes:

$$T = T_{max}\, e^{-mx}$$

The properties of the tube can be obtained by combining the properties of the fluid and the wall. Thus:

$$k_{eff} = \frac{k_w A_w + k_f A_f}{A_f}$$

Where:

k_{eff} - effective conductivity of the tube

k_w - wall conductivity

k_f - fluid conductivity

A_w - wall cross-section

A_f - fluid cross-section

A_T - tube total cross-section

Similarly:

$$(\rho\, Cp)_{eff} = \frac{(\rho\, Cp)_w A_w + (\rho\, Cp)_f A_f}{A_T}$$

$$\alpha_{eff} = \frac{k_{eff}}{(\rho Cp)_{eff}}$$

For a copper tube with water inside and:

$$d_T = 0.500 \text{ inches}$$

$$d_f = 0.450 \text{ inches}$$

$$k_w = 200 \frac{BTU}{Hr\ Ft°F}$$

$$k_f = 0.3 \frac{BTU}{Hr\ Ft°F}$$

$$(\rho Cp)_w = 559 \frac{\#}{Ft^3} \times 0.0915 \frac{BTU}{\#°F}$$

$$(\rho Cp)_f = 62.4 \frac{\#}{Ft^3} \times 1.0 \frac{BTU}{\#°F}$$

From McAdams h for a 1/2 inch pipe combining free convection and radiation is approximately:

$$h \sim 2 \frac{BTU}{Hr\ Ft^2 °F}$$

For the unit tested, the heat input was:

$$q = 500 \text{ milliwatts}$$

$$= 1.7 \text{ BTU/Hr}$$

Solving for T_{max}:

$$T_{max} = 7.3°F$$

This agrees well with the measured data. For this condition we also have:

$$m = 2.23 \text{ ft}^{-1}$$

so that no significant drop in temperature would be expected in the fraction of an inch which separates the probes.

H. Response to Flow

The moving source equations unfortunately do not strictly apply to the present case when flow occurs. This is because the source of heat moves with respect to the water, which comprises about 4/5 of the thermal mass, but is stationary with respect to the wall. Direct solution of the exact differential equations was felt to be beyond the scope of the present effort. An estimate was made, however, of the range of velocities which would be significant in altering the temperature distribution.

Maximum Estimate

If the wall were moving with the stream, but the probes were stationary, we would have:

$$m = 2.23\ Ft^{-1}$$

$$\alpha = 0.6345\ Ft^{2}\ Hr^{-1}$$

Then the velocity term would be comparable to the heat loss term when:

$$v = 2\alpha m$$

$$= 2.82\ Ft/Hr$$

This corresponds to a flow of Q = 88 cc/Hr

Minimum Estimate

If the wall were not only stationary, but also isothermal or non-conducting axially, acting to carry the lost heat to the outside, the heat loss to the wall would have a Nusselt Number of 4 (this is typical for developed laminar pipe flow).

Then:

$$h_w = \frac{4k_f}{d_f} = 23\ \frac{BTU}{Hr\ Ft^{2}\cdot F}$$

But since the ultimate loss is to ambient, this wall coefficient is in series with the previous value of h = 2, so that the overall coefficient corrected for circumference is:

$$h_o = 2.03$$

Using the water properties alone:

$$m = 26.9\ Ft^{-1}$$

$$\alpha = 5 \times 10^{-3}\ Ft^2/Hr$$

$$v = 2\alpha m$$

$$= 0.269\ Ft/Hr$$

which corresponds to a flow of:

$$Q = 8.4\ cc/Hr$$

In either case, it appears clear that the effects of flow on the temperature distribution will become evident at flow rates near the low leakage limit.

REFERENCES

Fuchs, N.A., Evaporation and Droplet Growth in Gaseous Media. Pergamon Press, 1959.

McAdams, W.H., Heat Transmission. McGraw-Hill, pp 267, pp 179, 1954.

Jakob, M., Heat Transfer. Volume I, Wiley, 1949, pp 346.